

8-2020

## BST2 ISOFORMS: DISTRIBUTION AND POTENTIAL USE IN CANCER THERAPEUTICS

Ahmed Muhsin

Follow this and additional works at: [https://digitalcommons.library.tmc.edu/utgsbs\\_dissertations](https://digitalcommons.library.tmc.edu/utgsbs_dissertations)



Part of the [Medicine and Health Sciences Commons](#)

---

### Recommended Citation

Muhsin, Ahmed, "BST2 ISOFORMS: DISTRIBUTION AND POTENTIAL USE IN CANCER THERAPEUTICS" (2020). *The University of Texas MD Anderson Cancer Center UTHealth Graduate School of Biomedical Sciences Dissertations and Theses (Open Access)*. 1021.

[https://digitalcommons.library.tmc.edu/utgsbs\\_dissertations/1021](https://digitalcommons.library.tmc.edu/utgsbs_dissertations/1021)

This Thesis (MS) is brought to you for free and open access by the The University of Texas MD Anderson Cancer Center UTHealth Graduate School of Biomedical Sciences at DigitalCommons@TMC. It has been accepted for inclusion in The University of Texas MD Anderson Cancer Center UTHealth Graduate School of Biomedical Sciences Dissertations and Theses (Open Access) by an authorized administrator of DigitalCommons@TMC. For more information, please contact [digitalcommons@library.tmc.edu](mailto:digitalcommons@library.tmc.edu).

BST2 ISOFORMS: DISTRIBUTION AND POTENTIAL USE IN CANCER  
THERAPEUTICS

by

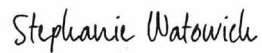
Ahmed Mohammed Muhsin, MBChB MPH

APPROVED:



---

Laura Bover, Ph.D.  
Advisory Professor



---

Stephanie Watowich, Ph.D.



---

Shao-Cong Sun, Ph.D.



---

Jagannadha Sastry, Ph.D.



---

Robert Orlowski, M.D., Ph.D.

APPROVED:

---

Dean, The University of Texas  
MD Anderson Cancer Center UTHealth Graduate School of Biomedical  
Sciences

BST2 ISOFORMS: DISTRIBUTION AND POTENTIAL USE IN CANCER  
THERAPEUTICS

A

THESIS

Presented to the Faculty of  
The University of Texas  
MD Anderson Cancer Center UTHealth  
Graduate School of Biomedical Sciences  
in Partial Fulfillment  
of the Requirements  
for the Degree of  
MASTER OF SCIENCE

by

Ahmed Mohammed Muhsin, MBChB MPH

Houston, Texas

August, 2020

## **Dedication**

This research work is dedicated to my role model for professionalism, the person who fed me the love of science since childhood and taught me that nothing is impossible with research... my father Professor Mohammed Muhsin.

This thesis is also dedicated to the most caring, loving and amazing woman in my life, my mother.

Lastly, without her patience and unlimited support, this research would never happen. To my wife and soulmate, Hawraa, I hope you liked this work ... and please buckle up, I am going to start my PhD soon... I love you!

## **Acknowledgments**

There is not an enough way to express my appreciation and gratitude to my advisor, Professor Bover, for all her guidance, teaching and support during the past three years I spent at the Monoclonal Antibody Core facility. Since I first heard about it in 1997, I was fascinated by the hybridoma technology and eagerly wanted to know every aspect about it. My dream came true and I was so lucky to learn this technology here at MD Anderson Cancer Center, and under the supervision of Dr. Bover, who herself received first-hand training from the inventor of this technology and the Nobel Prize winner, Dr. Milstein.

With no other graduate students or postdocs in the core facility, the training and assistance I received from the lab members were crucial for my success. I deeply want to thank our laboratory manager, Long Vien, who taught me every step in the hybridoma generation, from immunization to subcloning. I also want to thank Mrs. Janis Johnson for assisting me in the purification process and Julio Pollarolo for teaching me the various methods of ELISA. Lastly, I truly appreciate the invaluable encouragement and support from Felipe Amaya-Manzanares and Zhuang Wu. I will miss you all.

I want to express my sincere appreciation to the members of my advisory committee for their guidance and time. Professors Robert Orlowski, Stephanie Watowich, Jagannadha Sastry and Shao-Cong Sun, thank you all so much.

I am truly grateful to the core facilities at MD Anderson Cancer Centers for the training and assistance in running experiments. I would like to thank the faculty and

staff at the Advanced Cytometry & Sorting Facility at South Campus (ACSF), especially Karen Ramirez, Sarah Schneider and Veena Papanna. I would also like to thank the scientists at the Functional Genomic Core, Dr. Yutong Sun and Dr. Chien-Chia Cheng, for their help and training in the BST2 Knockdown project.

Lastly, I am very thankful to Dr. Inés Bravo at the Laboratory of Molecular Pathology, Hospital El Cruce, Florencio Varela, Buenos Aires, Argentina for performing immunohistochemistry assays on human breast cancer tissues, using the generated monoclonal antibody (anti-BST2-long clone LA5).

## **Abstract**

### **BST2 ISOFORMS: DISTRIBUTION AND POTENTIAL USE IN CANCER THERAPEUTICS**

Ahmed Mohammed Muhsin, MBChB MPH

Advisory Professor: Laura Bover, Ph.D.

Identifying a cancer-specific cellular target is one of the key factors that can pave a “bench to the bedside” path of a target therapy. Bone marrow stromal cell antigen 2 (BST2) is a raft-associated type II transmembrane protein with an unusual topology. Analyses showed a variable degree of BST2 expression in most organs. Two research groups identified different BST2 isoforms of BST2 generated by posttranscriptional modification. In this research, I studied the long BST2 isoform’s distribution in breast tissue and B cell lines using the novel monoclonal antibody (MAb) LA5, an anti-BST2-long MAb. This approach revealed the expression of the long BST2 isoform in the malignant B-cell lines. Moreover, immunohistochemistry staining of ductal breast carcinoma tissues showed the ability of the generated MAb to detect long BST2-positive cancer cells surrounded by negatively stained normal tissue, indicating LA5 specificity for this isoform. In contrast to the existing clone 26F8 that binds to all isoforms, the LA5 MAb specifically recognized malignant cells while distinguishing and excluding surrounding normal cells. The specificity of the generated MAb clearly demonstrates potential diagnostic value in detecting the early infiltrations of malignant breast ductal carcinoma in specimens collected from

patients. The other segment of my research entailed exploring the roles of BST2 in breast cancer, using a loss-of-function approach with BST2-targeting short hairpin RNA (shRNA) in the T47D breast cancer cell line. Silencing BST2 was associated with a statistically significant reduction in the viability of T47D (p value < 0.05) but had no impact its proliferation (p value = 0.6). Lastly, the downstream effects of BST2 silencing was evaluated through reverse phase protein array (RPPA) and revealed the statistically significant upregulation of four genes: MAPK1/MAPK3, HES1, FN1 and STAT3 (p value < 0.05). All these genes play different roles in the survival mechanisms that breast cancer cells may initiate when a critical pathway becomes compromised. By examining the adaptive cellular responses to BST2 silencing, this study offers insight into potential gene expression changes in breast cancer cells, with some changes enhancing the survival and proliferation of malignant cells.



## **Table of Contents**

<b>Approvals .....</b>	<b>i</b>
<b>Title .....</b>	<b>ii</b>
<b>Dedication .....</b>	<b>iii</b>
<b>Acknowledgements .....</b>	<b>iv</b>
<b>Abstract .....</b>	<b>vi</b>
<b>List of Figures .....</b>	<b>xii</b>
<b>List of Tables .....</b>	<b>xiv</b>
<b>Introduction .....</b>	<b>1</b>
1.1 What is BST2? .....	1
1.2 BST2 Structure .....	1
1.3 Physiological Roles of BST2.....	2
1.3.1 Pre-B Cell growth.....	2
1.3.2 Monocyte adhesion to endothelial cells .....	3
1.3.3 Antiviral role.....	3
1.3.4 Immunomodulation .....	3
1.4 BST2 Distribution .....	5

1.4.1 Normal tissues .....	5
1.4.2 Cancer tissues .....	7
1.5 BST2 Isoforms .....	11
1.6 Hypothesis .....	13
1.7 Specific Aims .....	15
<b>Materials and Methods</b> .....	16
2.1 Antigen for Mice Immunization .....	16
2.1.1 Injection doses preparation .....	16
2.2 Animal Work .....	16
2.2.1 Tail vein blood collection.....	16
2.2.2 Immunization route and schedule.....	17
2.2.3 Euthanasia .....	17
2.2.4 Harvesting the popliteal lymph nodes .....	17
2.3 Hybridoma Generation .....	17
2.4 Hybridomas Colony Pickup .....	19
2.5 ELISA Screening .....	20
2.6 Flow Cytometry Staining and Analysis (FACS) .....	21
2.7 Hybridoma Subcloning .....	22

2.8 Purification and Concentration of the MAbs .....	22
2.9 Antibody Isotyping .....	23
2.10 Affinity Testing .....	23
2.11 Specificity .....	25
2.12 Cell Lines and Media .....	25
2.13 Immunocytochemistry and Immunohistochemistry .....	26
2.14 BST2 Silencing Using Short Hairpin RNA (shRNA) .....	27
2.14.1 Transduction of the cell lines .....	28
2.15 Cell Viability Assay .....	28
2.16 Cell Proliferation Assay .....	28
2.17 Reverse Phase Protein Array (RPPA) .....	29
2.18 Statistical Analysis .....	29
<b>Results .....</b>	<b>30</b>
3.1 Generating the Long BST2 Peptide, Immunization and Serum Titer.....	30
3.2 Fusion, Hybridoma Generation and ELISA Screening.....	33
3.3 Cell-Based ELISA .....	35
3.4 Flowcytometry Staining of HEK293 Cell Lines.....	37
3.5 Antibody Isotype .....	42

3.6 Antibody Affinity .....	43
3.7 Antibody Specificity.....	45
3.8 Flow Cytometry Staining of B Lineage and Breast Tissue Cell Lines.....	49
3.9 Immunohistochemistry Staining.....	53
3.10 BST2 Silencing via shRNA .....	59
3.11 Cell Viability Assay .....	62
3.12 Cell Proliferation Assay .....	63
3.13 Protein Expression in T47D Cell Lines pre- and post BST2 Silencing....	64
<b>Discussion &amp; Future Directions .....</b>	<b>68</b>
4.1 Discussion .....	68
4.2 Future Directions .....	77
<b>Bibliography .....</b>	<b>78</b>
<b>Vita .....</b>	<b>87</b>

## **List of figures**

Figure 1.1 The four components of BST2 Structure .....	2
Figure 1.2 The interaction between BST2 and ILT7 .....	4
Figure 1.3 BST2 RNA expression levels in various tissues and organs.....	6
Figure 1.4 BST2 protein expression levels in various tissues and organs.....	7
Figure 1.5 BST2 protein expression levels in various cancers.....	8
Figure 1.6 BST2 Isoforms as described by patent JP2004173767 .....	11
Figure 1.7 BST2 Isoforms as described by Cocka LJ, Bates P.....	12
Figure 3.1 Immunization schedule .....	31
Figure 3.2 Immune response .....	32
Figure 3.3 Dilutional assay .....	34
Figure 3.4 Cell-based ELISA .....	37
Figure 3.5 Flowcytometry staining of the HEK293 cell lines .....	38
Figure 3.6. Comparison between Clones LA5 and Clone26F8 .....	40
Figure 3.7 Anti-BST2-long MAb Screening Funnel .....	41
Figure 3.8 Isotype ELISA Test .....	42
Figure 3.9 Determination of $K_a$ , $K_{dis}$ and $K_D$ for LA5-antigen binding .....	43
Figure 3.10 Determination of $K_a$ , $K_{dis}$ and $K_D$ for 26F8-antigen binding.....	44

Figure 3.11 LA5 MAb specificity .....	46
Figure 3.12 26F8 MAb specificity .....	47
Figure 3.13 Specificity comparison of the LA5 and 26F8 .....	48
Figure 3.14 Flow cytometry staining of B cell lines .....	50
Figure 3.15 Flow cytometry staining of breast tissue cell lines .....	52
Figure 3.16 Immunohistochemistry staining of HEK293 cell lines .....	54
Figure 3.17 Immunohistochemistry slides of infiltrating ductal breast carcinoma surrounding normal acinus .....	56
Figure 3.18 Immunohistochemistry slides of infiltrating ductal breast carcinoma surrounding normal ducts .....	58
Figure 3.19 Flow cytometry dot plots of T47D cell lines .....	60
Figure 3.20 Cell viability assay .....	62
Figure 3.21 Cell proliferation assay .....	63
Figure 3.22 Heatmap of T47D cell lines .....	65
Figure 3.23 T47D upregulated genes after BST2 Silencing .....	66
Figure 3.24 T47D downregulated genes after BST2 Silencing .....	67

## **List of tables**

Table 1 Steps and times of the kinetics assay.....	24
--	----

## **Introduction:**

### **1.1 What is BST2?**

Bone marrow stromal cell antigen 2 (BST2) is a type II transmembrane protein, consisting of 180 amino acids (1). This protein was first described in 1994 by Goto et al. as a B-cell specific marker and was named HM1.24 antigen (2). Around the same time, another research group identified the BST2 gene, located on chromosome 19p13.2, which showed variable expression in most normal tissues (3). Later, it was found that HM1.24 and BST2 were identical. In 2008, Neil et al. identified the cluster of differentiation 317 (CD317) in different cell lines, with the same structure as BST2. In some viral infections, these molecules tie up or “tethers” virions to the interior of infected cells, so it also acquired the name “Tetherin” (4). The reported molecular weight of this protein is 30-36 kDa, but posttranslational modifications (e.g., ubiquitination) may raise the molecular weight to 70 kDa (5).

### **1.2 BST2 Structure**

The structure of BST2 protein consists of four parts: a cytoplasmic tail representing the amino terminal domain, a transmembrane domain, an extracellular domain and a glycosylphosphatidylinositol (GPI) anchor, which represents the protein's carboxyl terminal (6). Being attached to the plasma membrane by two structurally different anchors gave BST2 an unusual topology (Figure 1.1). The presence of the GPI anchor infers that the localization of BST2 is within the plasma membrane microdomain (7).



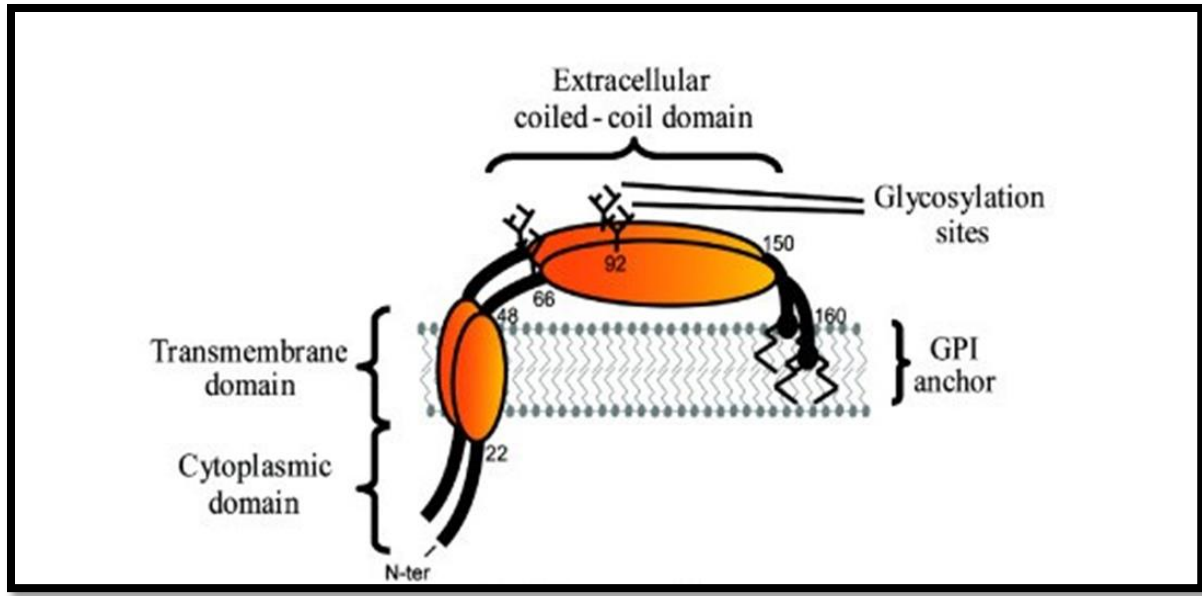


**Figure 1.1 The four components of BST2 structure.**

(Figure reproduced with permission from Dube M, Bego MG, Paquay C, Cohen EA. *Retrovirology* 2010, 7:114).

In the polarized epithelial cells, it was found that the distribution of BST2 is limited to the apical cell membrane, contrasting the pattern observed in B cells or in multiple myeloma, which consist of unpolarized cells (8). As shown in Figure 1.1, BST2 is assembled in dimers, through disulfide bonds. BST2 can also be found in the cytoplasm, mainly within the *trans* Golgi network (TGN), as a consequence of clathrin-mediated internalization from the surface, with data suggesting a continuous cycling of the protein between the cell membrane and the TGN (7).

### 1.3 Physiological Roles of BST2

**1.3.1 Pre-B cell growth:** only one reported finding suggests a possible role of BST2 in the expansion of Pre-B cells. It was based on the observation of the

enhanced growth and proliferation of DW34, a murine pre-B cell line, when co-cultured with BST2-positive BALB 3T3 cells, a murine fibroblast cell line. This report suggests that pre-B cells have a BST2 ligand for this cell-cell interaction (3).

**1.3.2 Monocyte adhesion to endothelial cells:** The expression of BST2 on the surfaces of many cells can be upregulated following interferon-gamma stimulation. Interferon-gamma, a type II interferon and a proinflammatory cytokine, is released by different immune cells as one of the host responses to infection or inflammation (9). Upon stimulation, the endothelial cells demonstrate an increased expression of BST2. BST2 thus acts as an adhesion molecule to monocytes and facilitates the migration of these cells out of the endothelium to the inflammatory site (10).

**1.3.3 Antiviral role:** As mentioned earlier, BST2, also known as Tetherin, has a demonstrated antiviral effect by binding virions particles to intracellular space, preventing viral budding. At first, this was observed in human immunodeficiency virus (HIV) which lacks the viral accessory protein, Vpu (4). However, later studies showed that the activity of this cellular restriction factor extends to other enveloped viruses, including retroviruses, filoviruses, herpesviruses and rhabdoviruses (11).

**1.3.4 Immunomodulation:** In response to an infection (or any nucleotide-containing stimuli), the plasmacytoid dendritic cells (pDCs) secrete copious amount of proinflammatory cytokines and chemokines, through the stimulation of its Toll-like receptors 7 and 9 (TLR 7 and 9), including type I interferons (IFN I), tumor necrosis factor (TNF) alpha and Interleukin 6. In paracrine fashion, IFNs will upregulate BST2 expression in cells within the vicinity of the pDCs. In turn, BST2 will interact with a

distinct receptor on the pDCs surface, called Immunoglobulin like transcript-7 (ILT7), resulting in the inhibition of IFN-alpha secretion on by pDCs (Figure 1.2). This interaction ensures the controlled secretion of cytokines and prevents adverse effects that could be associated with prolonged IFN stimulation (12).

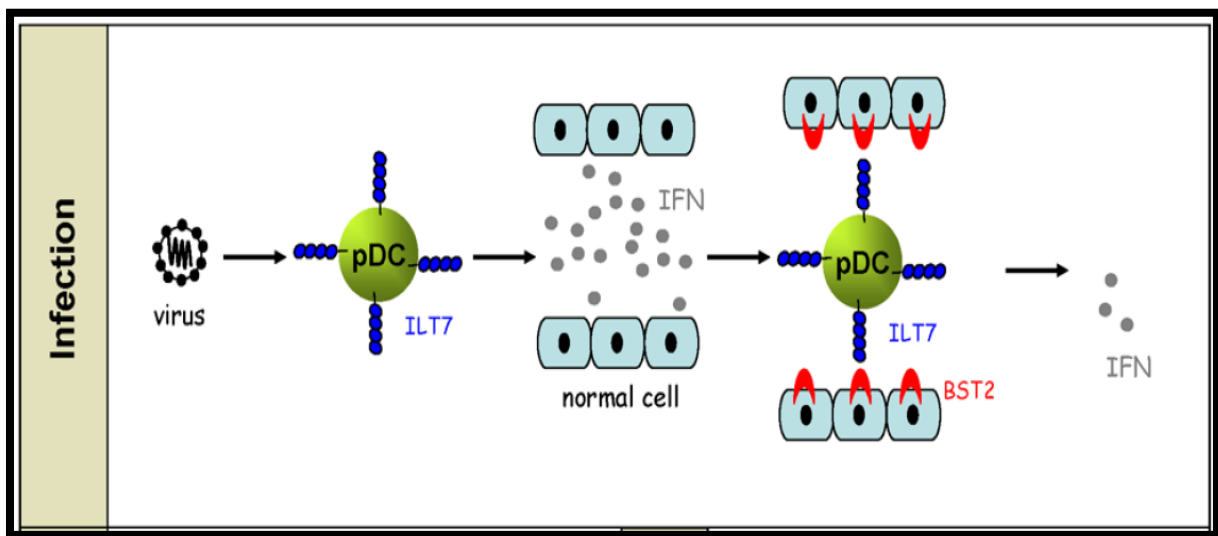


**Figure 1.2 The interaction between BST2 and ILT7.**

This interaction will reduce the secretion on IFN by pDCs and limit the impact in the host (Figure reproduced with permission from Cao and Bover. Immunol Rev. 2010 Mar; 234(1): 163–176).

The roles of BST2 in immunomodulation are not limited to the innate immune response. In experiments conducted by Urata et al., BST2-knock out mice demonstrated abnormal distribution of the viral nucleoprotein within the spleen. The dispersed virus was associated with defective T-cell priming and proliferation, with subsequent reduction in its effector functions (13). Moreover, the infected cells with Vpu-deficient HIV1 strains demonstrated enhanced clearance via antibody-

dependent cellular cytotoxicity (ADCC). With BST2 silencing, these infected cells showed reduced sensitivity to this type of adaptive immune response (14). The “tethering” activity of BST2 is not restricted to the viral envelope. Instead, it can tether a variety of exosomes, which are extracellular vesicles that engage in many functions, including antigen presentation. By tethering exosomes, BST2 can play a role in managing the limit of engagement of these exosomes in antigen presentation and dendritic cell activation (15). In addition, this function could have an implication on the host immune response within the tumor microenvironment. Lastly, upregulation of BST2 in many cancers, e.g., breast cancer, ovarian cancer, and melanoma, can suppress IFN secretion by the pDCs through interactions with ILT7. This interaction may attenuate the immune response against the tumor and play a role in tolerance to malignant growths (12). BST2 immunomodulatory effects thus involve both innate and adaptive immunity.

## **1.4 BST2 Distribution**

**1.4.1 Normal tissues:** When it was first described, BST2 was thought to have a preferential expression on terminally differentiated B cells (2), a finding that led to the use of this surface marker as a target for monoclonal antibody-based immunotherapy against multiple myeloma. However, using tissue microarray, later research studied the extent of BST2 expression in various human tissues and found a broad range of organs that expressed this protein, including the liver, pancreas, lungs, kidneys, and vascular endothelium. The pattern of BST2 expression (constitutive vs inducible) and its level in tissues and organs were widely variable and incompletely regulated by IFN I stimulation (16). The findings in this study are in

consensus with what has been reported in the Human Protein Atlas, which showed variable RNA and protein expression levels among the different organs and tissues (Figure 1.3 and 1.4) (17).

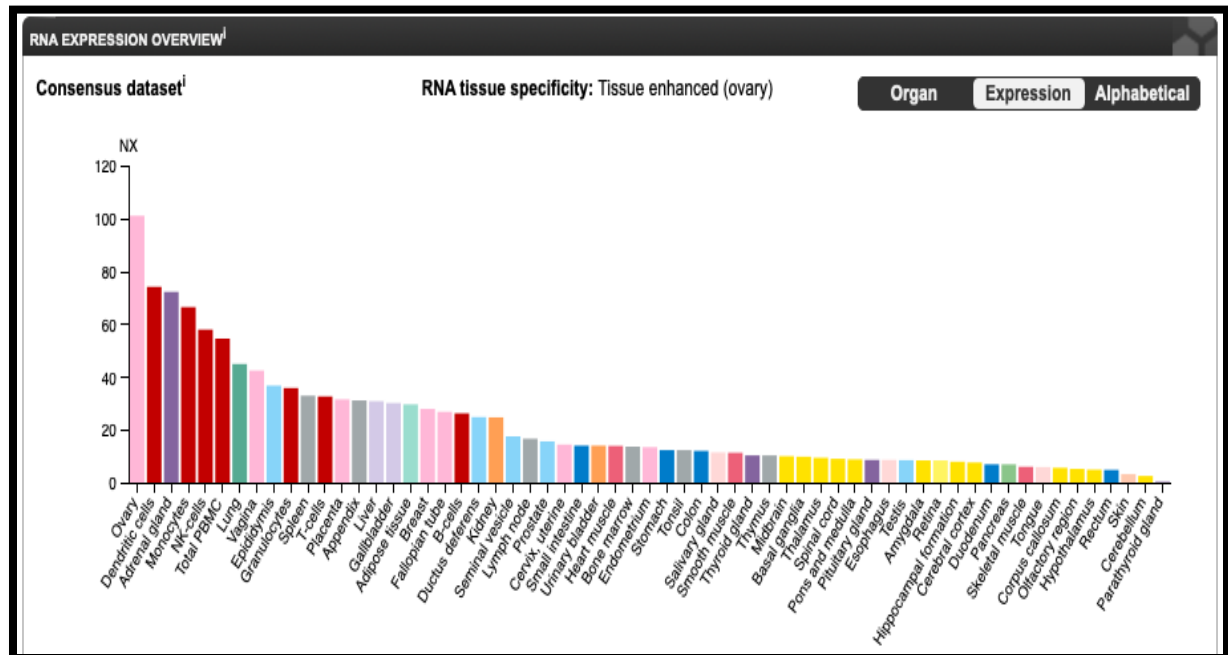


**Figure 1.3 BST2 RNA expression levels in various tissues and organs.**

Using RNA-Seq data from the Consensus dataset and the ovary as the tissue enhanced reference (Image credit: Human Protein Atlas version 19.1, BST2, <https://www.proteinatlas.org/ENSG00000130303-BST2/tissue>).

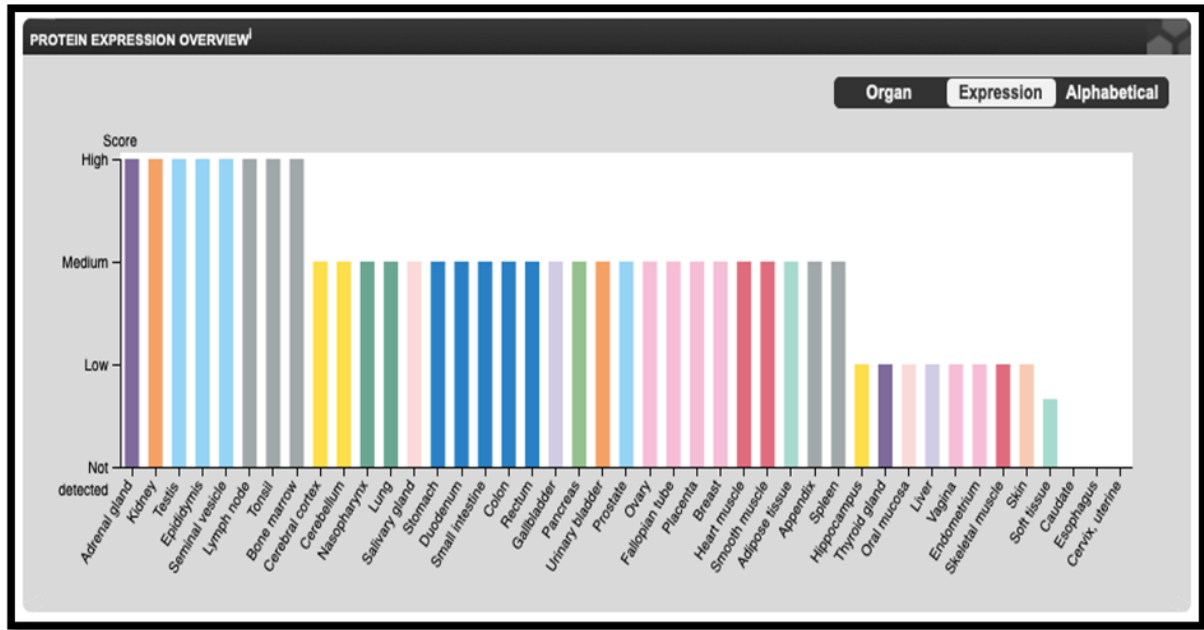


**Figure 1.4 BST2 protein expression levels in various tissues and organs.**

(Image credit: Human Protein Atlas version 19.1, BST2,

<https://www.proteinatlas.org/ENSG00000130303-BST2/tissue>)

**1.4.2 Cancer tissues:** The utilization of high-throughput molecular analysis techniques such as tissue microarrays and serial analysis of gene expression demonstrated the overexpression of BST2 in several solid and hematological malignancies at both the RNA and protein levels (18). During my study, I reviewed data from the Human Protein Atlas, which indicated that most examined cancer tissues stained positive with anti-human BST2 antibodies (Figure 1.5). The expression level was variable; high/moderate expression was observed in liver, breast, gastrointestinal and head and neck cancers, while low expression was noted in lymphoma and testicular cancers (17, 19).

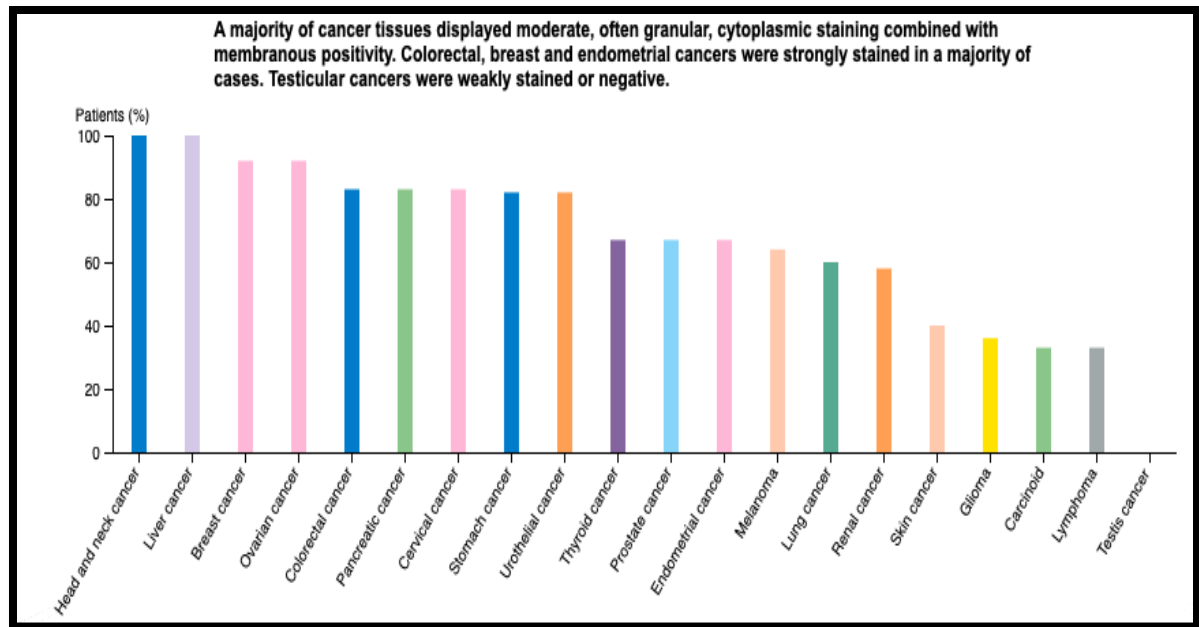


**Figure 1.5 BST2 protein expression levels in various cancers.**

(Image credit: Human Protein Atlas version 19.1, BST2,

<https://www.proteinatlas.org/ENSG00000130303-BST2/pathology>).

In breast cancer, a study found that the BST2 gene was upregulated in bone-metastatic breast cancer cell line, compared to other primary and non-bone metastatic breast cancer cell lines. Moreover, BST2 serum levels were statistically significantly higher in patients with bone metastasis. Induced expression of BST2 in a primary breast cancer cell line enhanced its proliferation and migration abilities (20). Another research group identified a demethylation process at the gene level that drives the overexpression of BST2 and enhances the metastatic abilities of the primary breast cancer, including its survival in the blood stream and lung colonization (21).

In lung cancer, the upregulated expression of BST2 was observed in different lung cancer cell lines: small cell lung cancer, lung adenocarcinoma, and non-small cell lung carcinoma. However, the role of BST2 expression on lung carcinogenesis and/or metastasis must be elucidated. The commercially available anti-BST2 monoclonal antibodies (MAbs) did not have a direct impact on the viability or proliferation of these cell lines, but were able to show both antibody-dependent cellular cytotoxicity (ADCC) and complement-dependent cytotoxicity; these MAbs demonstrated significant effectiveness in reducing tumor size and growth in murine models (18).

In gastrointestinal cancers, BST2 overexpression was observed in cell lines representing esophageal, stomach and colorectal malignancies. BST2 silencing was associated with significant reduction in cell growth, and overexpressing BST2 protein in a BST2-deficient colorectal cancer cell line significantly enhances its growth. Furthermore, the expression of BST2 was correlated with poorer survival among patients with gastrointestinal cancers (22).

In head and neck cancers, many gene expression databases indicated overexpression of BST2. Clinical data from patients with head and neck squamous cell carcinoma and high BST2 expression showed poor survival, compared to patients with low BST2 expression (23). Moreover, BST2 silencing rendered nasopharyngeal cancer cells sensitive to cisplatin and halted its resistance to platinum therapy (24).

Lastly, in hematological malignancies, BST2 (or HM1.24) was first described as a membrane glycoprotein in multiple myeloma and was thought to be selectively



expressed on terminally differentiated B cells. More than 80,000 molecules of BST2 could be identified on the surface of a single myeloma cell (2). Although the functional role of BST2 in multiple myeloma has not been identified yet, the overexpression of this surface protein and the need for new therapeutic approaches in treating this malignancy made BST2 a potential therapeutic target, using MAbs. Initial preclinical studies and mouse models demonstrated the effectiveness of these anti-BST2 MAbs in limiting the tumor burden, mainly through ADCC. Consequently, a phase I/II clinical study was initiated to test the safety and effectiveness of these MAbs as a therapeutic agent in patients with relapsed or refractory multiple myeloma. The response rate was relatively low, and the study was terminated, despite manageable adverse events (25). The expression of BST2 on the surface of other malignant blood cells, including mature B lymphocytes, has been evaluated as well. Using patients' samples, BST2 was expressed in chronic lymphocytic leukemia and mantle cell lymphoma, making BST2 a potential therapeutic target in other subclasses of malignancies (26).

To conclude, BST2 has been extensively investigated and studied for its protumor roles. It has been used as a target for new therapeutic approaches to treat different malignant diseases.

## 1.5 BST2 Isoforms

Different research groups described various BST2 isoforms resulting from alternative splicing. In 2005, a Japanese group identified three splice variants of BST2: BST2-D, BST2-H and BST2-HS (patent no. JP2004173767)(27). These variants differed in protein length and amino acid sequence. The isoforms were defined as followed: BST2-D (long isoform) is 180 amino acids, BST2-H (medium isoform) is 158 amino acids, and BST2-HS (short isoform) is only 100 amino acids (Figure 1.6). The functional significance of these variants and whether any of them are cancer-specific has not been studied and elucidation of their roles is warranted (27).

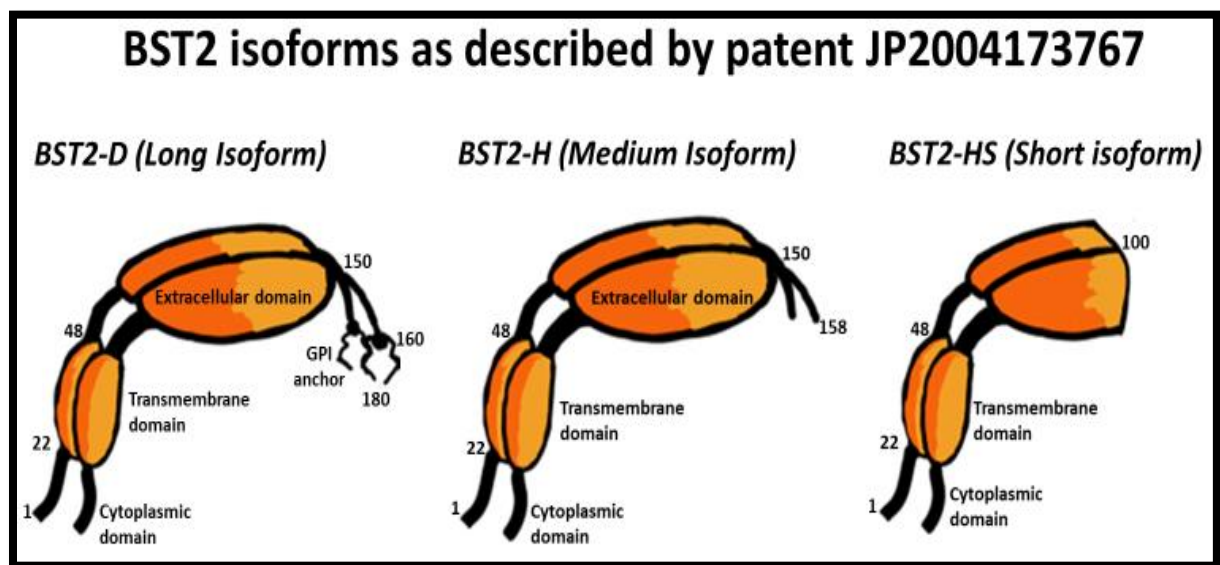


**Figure 1.6 BST2 Isoforms as described by patent JP2004173767.**

An illustration of the three isoforms described by the group of Japanese scientists: BST2-D (long isoform) with 180 amino acids, BST2-H (medium isoform) with 158 amino acids, and BST2-HS (short isoform) with 100 amino acids.

In 2012, Cocka et al. described two isoforms of Tetherin/BST2, a long isoform and a short isoform (28). As a consequence of alternative translation initiation, the short isoform was unrelated to that described earlier by the Japanese patent; it lacked the first 12 amino acids that present in the long isoform (Figure 1.7).

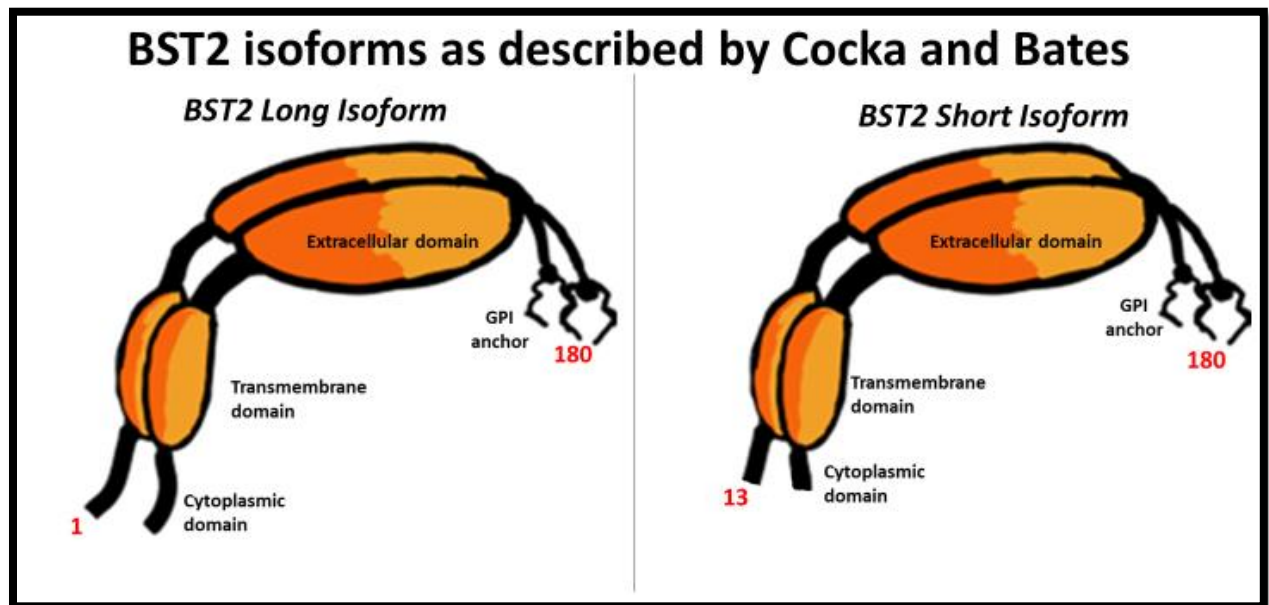


**Figure 1.7 BST2 Isoforms as described by Cocka LJ, Bates P.**

An illustration of the two isoforms described by Cocka et al. The long BST2 isoform has 180 amino acids and the short BST2 isoform has 168 amino acids, lacking the first 12 amino acids.

Cocka et al. demonstrated that these isoforms were associated with distinct antiviral and signaling activities. BST2 isoforms may merge with a similar or different isoform, forming homo- or heterodimers, respectively. Mechanisms that govern interactions between these isoforms to build dimers are not well understood, but the formation of homo- and heterodimers may have substantial effects on the functional

roles of BST2. Although both isoforms have the ability to restrict viral budding and release, through tethering the viral particles, the short isoform is more resistant to Vpu-mediated HIV antagonism. BST2 is a known activator of the Nuclear Factor-Kappa B (NF-kappa B) pathway, a signaling pathway involved in many biological activities, including the regulation of immune responses and inflammation (28). Unregulated activation of this pathway has been associated with carcinogenesis processes, including proliferation, migration, and invasion (29). The long BST2 isoform appeared as a potent activator of the NF-kappa B pathway, while the short isoform displayed no activation. Moreover, the short isoform exhibited an ability to modulate the effect of the long isoform on this pathway, and heterodimers demonstrated reduced NF-kappa B signaling. Increasing the number of short BST2 isoforms, relative to the long isoform, also diminished the activity of this pathway. This suggests the inhibitory role of the short isoform in regulating NF-kappa B pathway signaling by the long BST2 isoform (28).

## **1.6 Hypothesis**

Since my interest lies in cancer therapy, I decided to further study the isoforms proposed and patented by Jun Ohkawa and Yumiko Kakogawa. By collaborating with their group, our lab obtained the expression plasmids containing BST2-H (medium) isoform. The expression vector of the full-length BST2 (long BST2 isoform) was commercially available. HEK293 cells were previously transfected with these plasmids, and BST2 expression was confirmed via western blot analysis. Moreover, HEK293 cell lines expressing either long BST2 isoform (HEK293-long) or medium BST2 isoform (HEK293-medium) were recognized by the anti-BST2 MAb

(26F8) that was previously generated in our laboratory. Later, using a T-cell line with the nuclear factor of activated T cells - green fluorescent protein (NFAT-GFP) construct, our lab successfully integrated a human immunoglobulin like transcript 7 (ILT7) – Fc epsilon RI gamma protein (FCeRly) complex and created a report cell line that expresses GFP upon the interaction between ILT7 & and its ligand, BST2 (30). HEK293-long cells were able to activate NFAT, which resulted in GFP expression, while HEK293-medium cells failed to activate the reporter cell system.

In a prior experiment, using the same reported cell system, co-culturing the reporter cells with human breast carcinoma cell lines MDA-MB-468, MCF7, and T47D induced GFP expression. In contrast, other non-malignant cell lines known to express BST2 , such as HEK293, Vero and CHO, failed to induce GFP expression when co-cultured with the same reporter cells (31). Taken together, along with what has been described about the BST2 isoforms and their roles in activating or modulating NF-kappa B pathway, we hypothesized that:

- The long-reported isoform of BST2 (BST2 long) is preferentially expressed on cancerous cells and might be responsible for modulating the immune microenvironment by interacting with infiltrating immune cells like pDCs, and
- The expression of isoform H of BST2 (BST2 medium) might be restricted to normal cells.

## **1.7 Specific Aims**

Specific Aim 1: Generate anti-human-BST2 MAbs via hybridoma technology, specifically targeting the long BST2 isoform.

Specific Aim 2: Characterize the specificity of the antibodies and perform PK analysis of the selected purified clones to choose the best MAb candidates for immunohistochemistry (IHC) and for potential future therapeutic use.

Specific Aim 3: Use the generated anti-human-BST2 MAb candidates to analyze the expression of the long BST2 isoform in cancer and in normal tissues with flow cytometry staining and IHC.

Specific Aim 4: Study the function of BST2 in the T47D breast cancer cell line.

## **2. Materials and Methods**

### **2.1 Antigen for Mice Immunization**

A synthetic peptide was used as the antigen for immunization. It was produced by ThermoFisher Scientific in two forms, peptide alone and keyhole limpet hemocyanin (KLH)-conjugated peptide.

**2.1.1 Injection dose preparation:** The immunization doses were emulsified using incomplete Freund Adjuvant (IFA - InvivoGen). Using a 28-gauge insulin syringe, equal volumes of BST2-Long (D) peptide and IFA were mixed vigorously for several minutes until a white emulsion with maximum stability formed. Each emulsified 20 ul dose contained 10 ug of BST2-D peptide-KLH. On the three additional weekly boost injections, the peptide dose was raised to 15 ug.

### **2.2 Animal Work**

All animal experiments were conducted according to the University of Texas MD Anderson Cancer Center's Institutional Animal Care and Use Committee (IACUC) guidelines and approved protocols (Protocol IACUC 00000620-RN02). Female BALB/c mice were purchased from Jackson Laboratories (Bar Harbor, ME).

**2.2.1 Tail vein blood collection:** 50 ul of blood samples were collected from the lateral tail vein. It was punctured with a 28-gauge insulin needle while mice were restrained. After coagulation, serum was separated. An equal volume of glycerol was added to the serum and samples were stored at -20°C. A total of three serum samples were collected on day 0 (preimmunization), day 14 (after 5 injections) and day 31 after completing the schedule of immunization.

**2.2.2 Immunization route and schedule:** Three 6-8-week-old female BALB/c mice were immunized. On day 0, a 50 ul pre-immunization serum sample was collected from each mouse. Injections were given through a footpad route at three-day intervals (Day 0, 3, 6, 9, and 12) for a total of five injections. Three additional weekly injections were given to boost the immune response (Day 15, 22 and 29) to complete a grand total of 8 injections.

**2.2.3 Euthanasia:** Following MD Anderson IACUC guidelines, the mice were exposed to carbon dioxide (CO<sub>2</sub>) in the CO<sub>2</sub> chamber, at a flow rate of 2 L/min for six minutes. Cervical dislocation was performed as a secondary euthanasia method.

**2.2.4 Harvesting the popliteal lymph nodes:** After euthanasia, the mice were whipped with ethanol 70%, transferred to the tissue culture hood and pinned into a dissection board. Using scissors, a midline incision was made, and the fur was removed. The popliteal lymph node, located at the popliteal fossa and embedded in adipose tissue, was carefully excised to preserve the node structure and integrity. Only the popliteal lymph nodes draining the injected footpad were collected and placed in a petri dish with RPMI 1640 medium.

## **2.3 Hybridoma Generation**

The two mice with the highest serum titers were selected for fusion while the third mouse was reserved as a backup. The following materials and media were used:

- HAT supplement (50x) [Sigma]: this mixture of hypoxanthine (5 mM), aminopterin (20 µM) and thymidine (0.8 mM) was used to prepare the HAT



selection medium against unfused or self-fused SP2/0 myeloma cells. As a folic acid inhibitor, aminopterin blocks the de novo pathway for nucleoside synthesis in SP2/0 myeloma cells, which lack the hypoxanthine-guanine phosphoribosyl transferase (HGPRT) enzyme and, as such, they lose the ability to utilize nucleotides provided by the salvage pathway.

- RPMI 1640 medium [Sigma]: used to prepare the selection medium and washing cells.
- Polyethylene glycol (PEG 1450): used as the fusing agent in the hybridoma technique. On the day of fusion, 1 ml vial of PEG was maintained at 37°C until the fusion step.
- Rat Supplement (RSCM), used as a growth supplement for the hybridomas.
- Fetal Bovine Serum (FBS).

The selection media consists of RPMI – 1640 with 10% FBS, 2% HAT supplement 50x, and 3% RSCM. The following cells were used during the hybridoma generation experiment:

- SP2/0: The myeloma cell line SP2/0 was selected as a partner cell line for hybridoma generation. One week before fusion, SP2/0 murine myeloma cells were thawed, maintained in RPMI 1640 and 10% FBS and expanded to  $1 \times 10^8$  cells in petri dishes. On the day of fusion, cells were collected in 50 ml tubes, centrifuged, and washed twice with RPMI medium before the fusion process.
- Murine lymphocytes: These cells were collected from the excised popliteal lymph nodes. These lymph nodes were dissected with scissors and forced through a sterile stainless-steel strainer, to collect the cells in RPMI medium.

The collected lymphocytes were centrifuged (1000 RPM for three minutes) and washed twice with RPMI medium before the fusion process.

With a cell-counting hemocytometer, both SP2/0 and murine lymphocytes were counted and combined in a ratio of 1:2 (Sp2/0 to lymphocytes) in a 50 ml tube. The tube was centrifuged at 1000 RPM for five minutes to pack the cells together and prepare them for the fusion. After discarding the supernatant and loosening the cell pellet, 1 ml prewarmed (37°C) PEG was added to the tube while swirling for 45 seconds. The reaction was stopped by adding 24 ml prewarmed (37°C) RPMI medium. Fused cells were centrifuged at 1000 RPM for 5 minutes, supernatant was discarded, and the cell pellet was loosened by gentle tapping and transferred to the selection medium. Hybridoma cells suspension was distributed into six 96 MW plates (150 ul/well) and incubated at 37 °C, 5% CO<sub>2</sub>.

## **2.4 Hybridomas Colony Pickup**

Seven days after fusion, enzyme-linked immunosorbent assay (ELISA) was performed to detect positive wells containing hybridoma colonies. Following results, the procedure of “single colonies pickup” was performed in two phases at a one-week interval. Well-demarcated colonies were identified, collected with a 2 ul pipette, and transferred into a 96-well plate containing hypoxanthine and thymidine (HT) selection media. These colonies were incubated at 37°C and 5% CO<sub>2</sub>. A total of 563 colonies were picked up in two phases:

- Phase I: 284 colonies

- Phase II: 279 colonies

After two days, primary screening was performed via ELISA.

## **2.5 ELISA screening**

To select the hybridomas capable of producing specific monoclonal antibodies against the Long BST2 peptide, ELISA was performed. ELISA plates were coated with a 100- $\mu$ l coating buffer, containing the BST2-D peptide in a concentration of 1  $\mu$ g/ml, and incubated overnight at 4°C. The next day, ELISA plates were washed three times with PBSt (PBS containing 0.05% v/v Tween®-20) and blocked with 100  $\mu$ l of blocking buffer (PBS, 1% w/v BSA). After an hour of blocking at room temperature, 50  $\mu$ l supernatant from each of the 563 colonies were added to individual wells as the primary antibodies. The anti-BST2 MAb (clone 26F8) [eBioscience] was used as a positive control and blank wells with secondary antibody only were performed in triplicates. After one hour of incubation, three washes followed. 50  $\mu$ l of secondary antibody, goat anti-mouse IgG, HRP conjugated (1:2000) was added to each well and incubated for one hour. After washing four times, the substrate solution (TMB) was added to each well and incubated for 30 minutes. The reaction was stopped with H<sub>2</sub>SO<sub>4</sub> 0.2N and the OD absorbance values were read at 450 nm. This screening step was repeated twice. 26 hybridomas were transferred to 24-well plates containing HT-medium, and incubated for 4-7 days at 37°C, 5% CO<sub>2</sub>. 2 ml supernatant was collected from each clone for further MAb characterization.

For ELISA dilution assay, ELISA plates were coated overnight with 0.5 ug/ml BST2-D peptide; serial dilutions of the pre-collected supernatants were used as primary antibodies (undiluted, 1/15, 1/225 and 1/3375). The clones with the highest OD 450 nm signal were selected to proceed to the next screening assays.

For cell-based ELISA, plates were loaded with parental HEK293 cells, HEK293 expressing long BST2 isoform, or HEK293 expressing medium BST2 isoform at a density of  $15 \times 10^4$ /50 ul per well and dried at RT overnight. ELISA was performed as described before using 50 ul supernatant from each clone.

## **2.6 Flow Cytometry Staining and Analysis (FACS)**

For flow cytometry assays, cells were detached using 0.05% trypsin-EDTA, counted, washed, and resuspend with FACS Buffer (PBS, 2% FBS, 2 mM EDTA).  $2 \times 10^5$  cells in 100 ul/well were placed in a U-bottom 96-well plate and centrifuged (1000 RPM/ 3 min/ 4°C). The buffer was discarded and 100 ul of the previously collected supernatants were added to the wells and incubated on ice for 30 minutes. After incubation, the plate was washed three times with FACS buffer and 50 ul of diluted (1/250) secondary antibody (donkey anti-mouse allophycocyanin (APC) conjugated) were added to the wells and incubated on ice for 20 minutes while protected from light. The final wash was repeated four times, and the samples were transferred and analyzed at the South Campus Flow Cytometry & Cell Sorting Core Laboratory at MD Anderson Cancer Center. FACS data were analyzed with FlowJo™ Software-for Windows (Version 10.6.1. Ashland, OR: Becton, Dickinson and Company; 2020).

## **2.7 Hybridoma Subcloning**

The hybridoma clone (LA5) was expanded in 24 well plates with HT-based media for three days. With 70% confluency and viability of over 90 %, cells were counted (with a hemocytometer), and diluted to a concentration of 5 cells/ml. Using a multichannel pipet, 200 ul/well were added in a 96-well tissue culture plate. The hybridomas were cultured for 7-10 days at 37°C, 5% CO<sub>2</sub>. As described before, screening was performed by ELISA against the long BST2 peptide. The absorbance values were read at 450 OD, and the two wells with the highest OD signals were maintained and transferred into a 24-well plate. Two days later, the HT-based medium was substituted with RPMI-FBS 10% and the clones were transferred to T25. Further expansion into T75 was performed for the purpose of MAb purification.

## **2.8 Purification and Concentration of MAbs**

After expansion and incubation of the selected hybridomas, 300 ml of the MAb-rich supernatants were collected, centrifuged, and filtered through 0.45-micron membrane. MAbs were purified via Protein A affinity chromatography procedure (GE Healthcare MabSelect SuRe Cat # 17-5438-08). After the assembly and washing of purification columns, supernatant was neutralized with 1 M Tris-HCl (pH 9) buffer and allowed to run in the columns twice. The captured antibodies were eluted from the columns, using elution buffer (0.1M glycine-HCl, pH 3) and the concentration was measured in the Nanodrop. An overnight dialysis in PBS (Fisherbrand Regenerated Cellulose Dialysis Tubing) was performed and the concentrated anti-long BST2 (clone LA5) MAb (1 mg/ml) was collected and stored at 4°C, ready for further characterization and cell assays.

## **2.9 Antibody Isotyping**

The isotype of the generated MAb was determined using Mouse Monoclonal Antibody Isotyping Reagents [Sigma-Aldrich, Catalog Number ISO2] following manufacturer recommendations. It is based on the ELISA technique.

## **2.10 Affinity Testing**

Using the Octet RED384 System, the kinetics of the generated MAb were tested and compared to the anti-BST2 (clone26F8) MAbs [eBioscience]. Developed by FORTEBIO and based on Bio-Layer Interferometry (BLI) technology, the Octet RED384 system can measure the affinity constant (KD) of an antibody with a range of 1 mM to 5 pM (32). The following materials and conditions were applied to the experiments:

- Sensor type: AMC (Anti-mouse IgG Fc capture) biosensor (part number 18-5088, ForteBIO).
- 10x Kinetics buffer: 10mM Phosphate, 150 mM NaCl, 0.02% Tween 20, 0.05% Sodium Azide, 1 mg/mL BSA (pH 7.4) (part number 18-5060, ForteBIO).
- Monoclonal antibodies: clones LA5 and 26F8 at a concentration of 5 ug/ml.
- Recombinant human BST2 protein (Catalog number 13370-H07H, Sino Biological).
- BST2 protein concentrations: a serial dilution of concentrations was used to measure the KD values of the monoclonal antibodies (1000, 500, 250, 125,

62.5, 31.25 and 15.625 nanomolar). The calculated nanomolar concentrations were based on the molecular weight of the BST2 protein.

- Assay steps and time: following the guidelines, Table 1 describe the steps of the assay and time spent in each step.
- Data Analysis: I used Octet Data Acquisition software V10.x to analyze the results. I used a 1:1 binding model, where both the association and dissociation phases were taken into consideration. Results were obtained after global fitting from the various concentrations of protein.

**Table 1 Steps and times of the kinetics assay using the Octet RED384 system**

<b>Assay step</b>	<b>Step name</b>	<b>Assay time (seconds)</b>
<b>1</b>	<i>Baseline</i>	<i>60</i>
<b>2</b>	<i>Loading</i>	<i>300</i>
<b>3</b>	<i>Baseline</i>	<i>300</i>
<b>4</b>	<i>Association</i>	<i>300</i>
<b>5</b>	<i>Dissociation</i>	<i>300</i>
<b>6</b>	<i>Regeneration</i>	<i>5</i>

## **2.11 Specificity**

A specificity assay was performed and analyzed via flow cytometry staining of MM1, a multiple myeloma cell line. In this assay, changes in the binding of the LA5 MAb to the BST2 receptor expressed on MM1 cell lines were assessed after:

- 10-minute preincubation with BST2 protein (5ug/ml).
- 10-minute preincubation with Spartan protein (5ug/ml).

Results were compared to the anti-BST2 Clone 26F8 MAb and mouse IgG1 isotype control (eBioscience, catalog #14-4714-82). FACS data was analyzed with FlowJo™ Software - for Windows (Version 10.6.1. Ashland, OR: Becton, Dickinson and Company; 2020).

## **2.12 Cell Lines and Media**

The following cell lines were used:

- B-LCL: a non-malignant B cell line that has been infected with Epstein-Barr virus to provide a continuous source of primary B cells [Astrarte Biologics]. These cells were maintained and expanded in RPMI 1640 medium, supplemented with 10% FBS.
- MM1: a multiple myeloma cell line that was generously provided by Dr. Robert Orlowski's laboratory. It represents malignant B-lymphoblasts that grow in suspension and as lightly attached cells. These cells were maintained and expanded in RPMI 1640 medium, supplemented with 10% FBS.
- U266: a multiple myeloma cell line that was generously provided by Dr. Robert Orlowski's laboratory. It represents malignant B-lymphocytes that



grow in suspension. These cells were maintained and expanded in RPMI 1640 medium, supplemented with 10% FBS.

- MCF-10A: a nonmalignant epithelial breast tissue cell line [ATCC]. This cell line grows in a special medium that was purchased from Lonza/Clonetics as a kit [MEGM, Kit Catalog No. CC-3150].
- MDA-MB-231: human breast adenocarcinoma cell line that was generously provided by Dr. Ze Tian. These cells grow in RPMI-1640 based medium, supplemented with 10% FBS.
- MCF7: human breast adenocarcinoma cell line that was generously provided by Dr. Ze Tian. These cells grow in Dulbecco's Modified Eagle's medium, supplemented with 10% FBS.
- T47D: human breast ductal epithelial carcinoma. Stocks of this cell line were available in our lab. These cells grow in RPMI-1640 based medium, supplemented with 10% FBS.

### **2.13 Immunocytochemistry and Immunohistochemistry**

The immunocytochemistry (ICC) assays on transduced cells overexpressing BST2 isoforms were performed by the Research Histology Core Laboratory (RHCL) at MD Anderson Cancer Center. Paraffin blocks were prepared from cell pellets of HEK293, HEK293 BST2-long and HEK293 BST2-medium. Briefly, all cell pellets were fixed in 4% formalin for 10 minutes, centrifuged and washed with PBS and resuspended in fresh PBS prior to submission to the Core. The pellets were embedded in paraffin with standard techniques. 5  $\mu$ m sections were cut and stained with the corresponding supernatants or purified antibodies. The ICC detection of

BST2 was performed with the DAB kit (DAKO). Hydrogen peroxide was used to deactivate intrinsic peroxidase. Antigen retrieval was performed in a water bath using citrate-EDTA buffer (10mM citric acid, 2mM EDTA, 0.05% Tween 20, pH 6.2). Sections were incubated with undiluted supernatant containing secreted anti-BST2 antibodies or with a purified antibody. As negative controls, immunostaining was performed by incubating samples with PBS instead of the primary antibody. After staining with DAB and counterstaining with hematoxylin, the slides were recorded using a digital camera. The immunohistochemistry assays on human breast cancer tissues was performed at the laboratory of Molecular Pathology, Hospital El Cruce, Florencio Varela, Buenos Aires, Argentina (Dr. Inés Bravo).

#### **2.14 BST2 Silencing Using Short Hairpin RNA (shRNA)**

The Functional Genomic Core (FGC), at MD Anderson Cancer Center, carries a human shRNA library that targets the entire human genome, including five plasmids that target human BST2. Through collaboration with the FGC, the five different BST2-silencing plasmids (as well as a non-silencing control) were introduced into E. coli strain DH5 $\alpha$ . This strain harboring a plasmid was inoculated into an ampicillin-containing LB media and cultured at 37°C in a shaker incubator overnight. The plasmids were extracted with QIAGEN Plasmid Plus Midi Kit. HEK-293T cells were used to generate shRNA-containing lentivirus using a third-generation lentiviral system. jetPRIME reagent was used as a transfection reagent [Polyplus transfection, reference number 114-15]. Lentivirus-containing supernatants were collected 24- and 48-hours post- transfection and concentrated [LentiFuge Viral Concentration Reagent, Collecta, Catalog # LFVC1].

**2.14.1 Transduction of the cell lines:** The first step in transduction was to set the experiment conditions. The following assays were performed:

- Lentiviral transduction titration assay.
- Polybrene toxicity assay.
- Puromycin titration assay.

2 - 3 \* 10<sup>5</sup> cells were seeded per well in a 6-well plate. 24 hours later, 40 ul of 4x lentivirus vector was added per well, which was based on the multiplicity of infection (MOI) of 5. To enhance transduction, polybrene was added in a concentration of 8 ul/ml. 48 hours post-transduction, 2 ug/ml Puromycin was added to each well as a selective antibiotic. 10 days post-transduction, BST2 expression was assessed, using western blot and flowcytometry staining.

## **2.15 Cell Viability Assay**

Cell viability assay was performed on cells following BST2 silencing, using CellTiter-Glo Luminescent (Promega, Catalog # G7570), following manufacturer protocol.

## **2.16 Cell Proliferation Assay**

Cell proliferation assay was performed on cells following BST2 silencing using XTT - Cell Proliferation Assay Kit (ThermoFisher Scientific, Catalog # X12223).

## **2.17 Reverse Phase Protein Array (RPPA)**

Samples of non-silenced and silenced BST2 cell lines were sent to the Reverse Phase Protein Array (RPPA) Core at MD Anderson Cancer Center for functional

proteomics studies. Cell pellets were prepared at our lab and stored at -80°C.

Protein extraction was performed at the RPPA core lab.

## **2.18 Statistical Analysis**

Statistical analyses were performed with FlowJo™ Software – for Windows (Version 10.6.1. Ashland, OR: Becton, Dickinson and Company; 2020) and/or GraphPad Prism Software version 7.00 (La Jolla, California) for Windows. Data sets were analyzed with Mann-Whitney U Test, Student T-Test or ANOVA test.

P values for comparisons between groups were determined and a value of less than 0.05 was interpreted as statistically significant.

### **3. Results**

#### **3.1 Generating the Long BST2 Isoform Peptide, Immunization and Serum Titer**

To generate MAbs specifically against the long isoform of BST2 (BST2-D), a unique sequence should be identified. By comparing the amino acid sequences of the different isoforms of BST2, we identified a section of the extracellular domain of the BST2 protein found exclusively in the long isoform and not in the other isoforms of BST2. This peptide spanned between amino acids 133 and 156 on the long isoform of the BST2, the number of residues being 24. The amino acid sequence of the generated peptide was EVERLRRENQVLSVRIADKKYYPS and had the following molecular characteristics:

- Molecular weight: 2949.32 g/mol
- Isoelectric point: pH 10
- Solubility: Good water solubility

Given the small size of peptide, the use of KLH as a carrier protein was selected to ensure an adequate immune response can be elicited after mice immunization.

Three female Balb /c mice 6-8 weeks old were selected for immunization. Pre-immunization samples were collected and a series of footpad injections were scheduled at a defined interval (Figure 3.1).

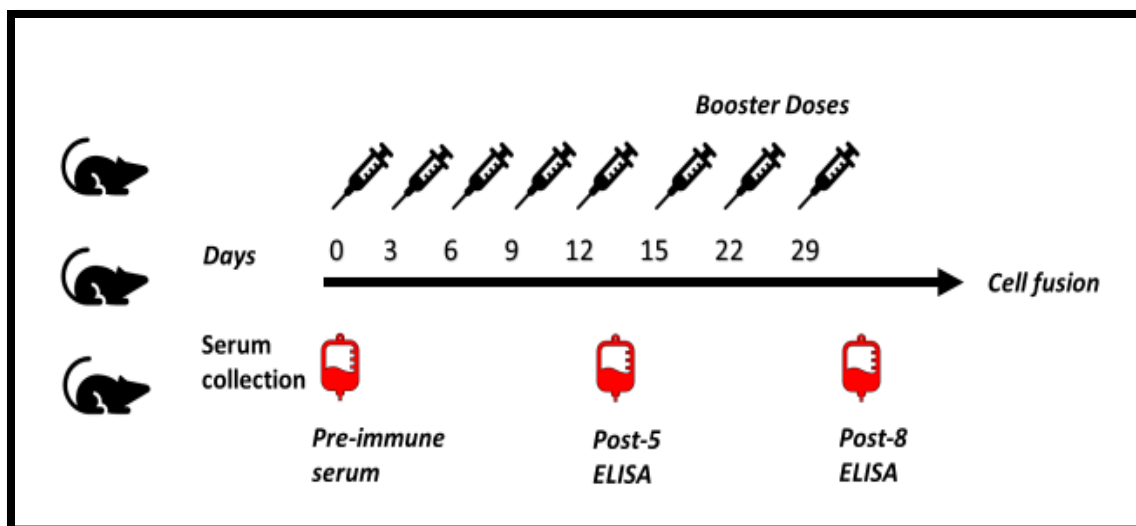


**Figure 3.1 Immunization Schedule.** Three mice were immunized every three days for the first five doses and then weekly for the three boosts doses. Blood samples were drawn at indicated times, following IACUC protocol 00000620-RN02.

Reasons for choosing the footpad route were the establishment of an easy and quick way to monitor the host immune response and the ability to collect a higher population of specifically-responding B lymphocytes to be used in the hybridoma technique, by harvesting the popliteal lymph nodes (33). To measure the immune response, serum titration was performed after five injections, using the ELISA technique. Results showed insufficient immune response. After the third weekly booster dose, serum titration assay was repeated and revealed an adequate immune response in each mouse to proceed with hybridoma generation by chemical fusion (Figure 3.2). Mice A and B were selected for the hybridoma experiment, while Mouse C was maintained as a backup source for reactive B lymphocytes.

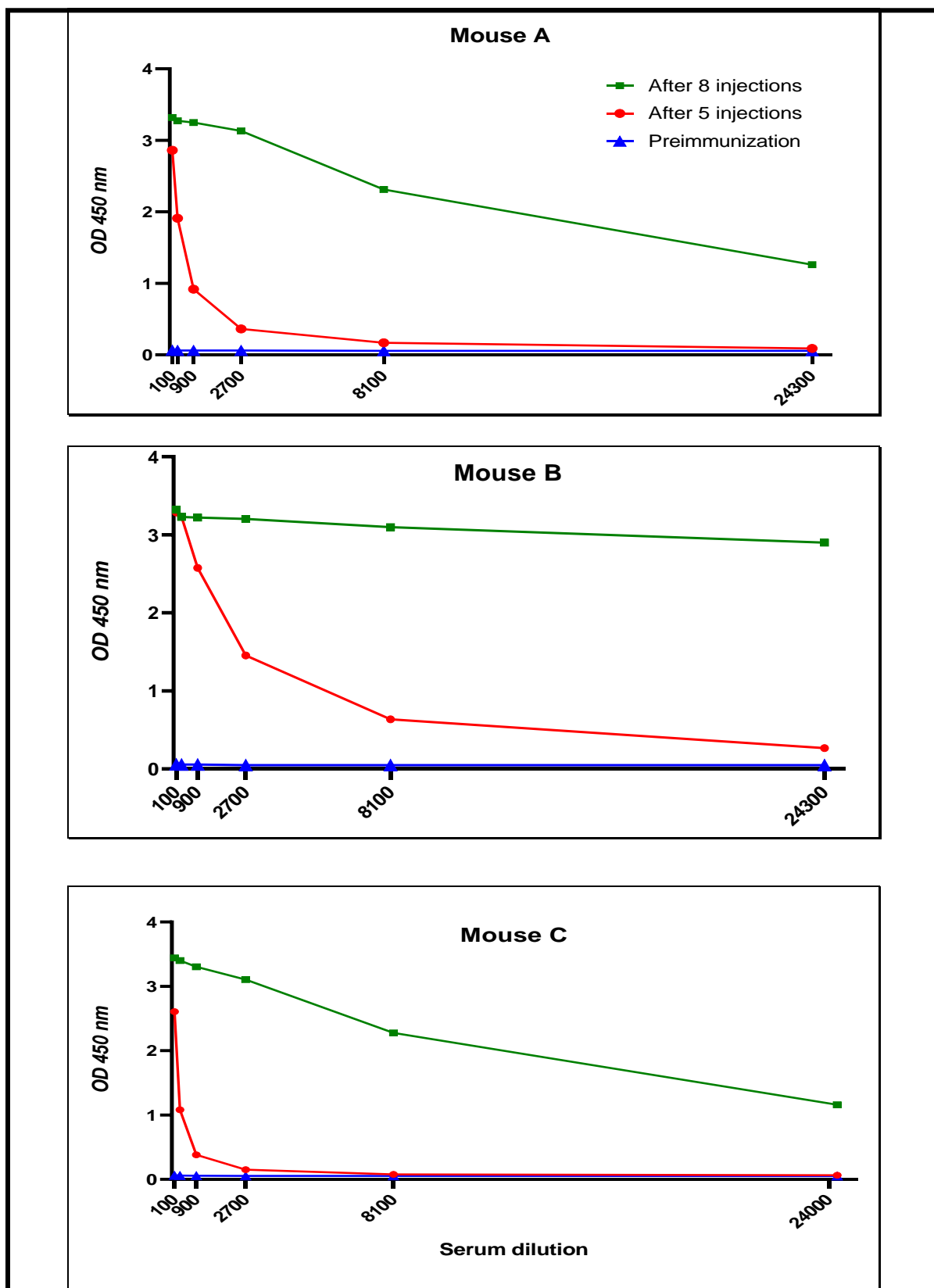


**Figure 3.2 Immune response.** Titration curves compare the immune response from the immunized mice (A, B and C) after five injections and then after eight injections. The pre-immune serum sample was used as a control. Plates were coated with BST2 peptide alone.

### **3.2 Fusion, Hybridoma Generation and ELISA Screening**

With an optimal serum titer observed two days after the last booster dose, fusion was performed on day 32. SP2/0 cells were selected as a partner cell line for hybridoma generation; these cells do not secrete immunoglobulins and are sensitive to the selection media HAT (hypoxanthine-aminopterin-thymidine). Within two weeks after fusion, I was able to identify 563 hybridomas in six 96-well plates. Initial ELISA screening of the 563 colonies generated by cell fusion revealed the presence of 26 clones with antibody-containing supernatant that is reactive against the peptide of interest (BST2-D peptide). To choose the best candidates among the selected colonies in terms of the productivity and affinity of the generated MAbs, a dilution assay was performed with the positive supernatants using the ELISA technique. The 16 clones with the highest OD 450 nm signal were chosen to proceed to the next screening assays (Figure 3.3).



## Dilution assay via ELISA

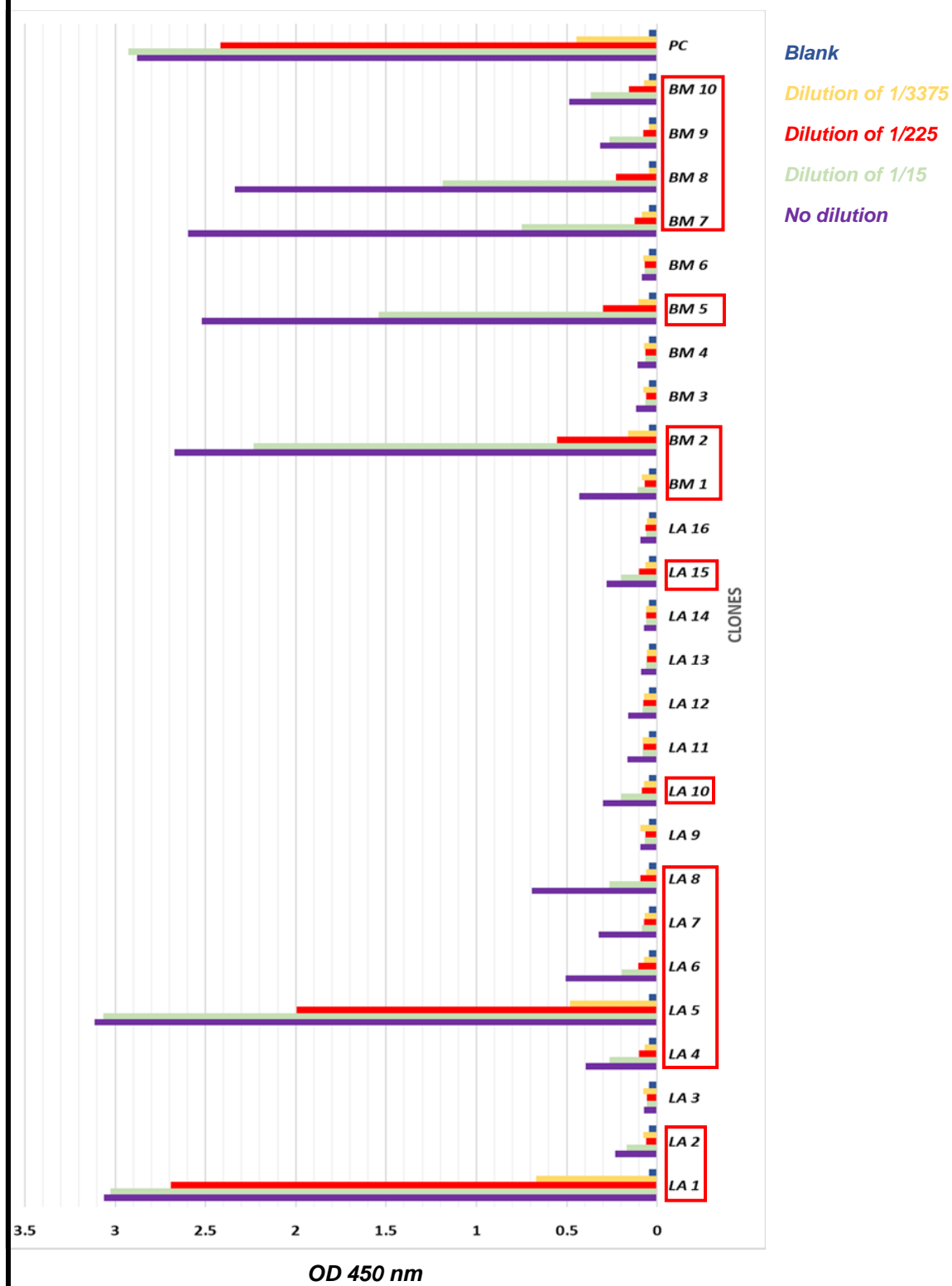


**Figure 3.3 Dilution assay.** 26 positive clones were tested at serial dilutions as described under the methods. Sixteen clones with the highest OD450 nm signal (red squares) have been selected for further characterization. LA1-LA16 were clones picked at the first round of colony pickup; clones BM1-BM10 were picked at the second round of colony pickup. PC (positive control) was anti-BST2 MAb (clone 26F8) 1 ug/ml which recognizes all isoforms. Plates were coated with BST2 peptide alone.

### 3.3 Cell-Based ELISA

Cell-based ELISA confirmed the ability of the generated hybridomas to secrete MAbs that specifically bind to the long isoform of BST2 (BST2-D) with minimal or no binding to the medium isoform (BST2-H). For that purpose, we used HEK293 cell line and transfectants previously generated in our laboratory. In summary:

- HEK293 (parental): These cells demonstrate a very low expression of BST2, and it is inducible using IFN.
- HEK293 WT-BST2 (or HEK293 long): the HEK293 cells are transfected with a plasmid of the full length BST2, which is identical to the long isoform of BST2. This transfectant constitutively expresses BST2 (non-inducible). A full length BST2 vector was commercially available.
- HEK293-H (or HEK293 medium): HEK293 cell line transfected with a plasmid that has the sequence of the medium isoform of BST2. The plasmid was

obtained through collaboration with Dr. Naoko Arai's laboratory, (SBI Biotech Co., Ltd., Ginkgo Biomedical Research Institute, Kawasaki 216-0001, Japan).

Both transfectants were recognized by anti-BST2 (26F8) MAb [eBioscience]. I selected the colonies that demonstrated maximum binding to the HEK293 cells expressing the long isoform (HEK293 BST2-long) and minimal interactions with the HEK293 parental or the HEK293 BST2-medium transfectant. The best three clones that met these criteria, reflected by their associated OD 450 signals, were chosen for the last stage of testing (Figure 3.4). LA1, LA5 and BM7 showed the best combination of high OD 450 signals with HEK293 BST2-long transfectants AND low signals with HEK293 BST2-medium and HEK293 cell lines, suggesting the capabilities of these clones to produce antibodies with high affinity to the long isoform of BST2, with minimal or no interaction to the other isoforms of this receptor.

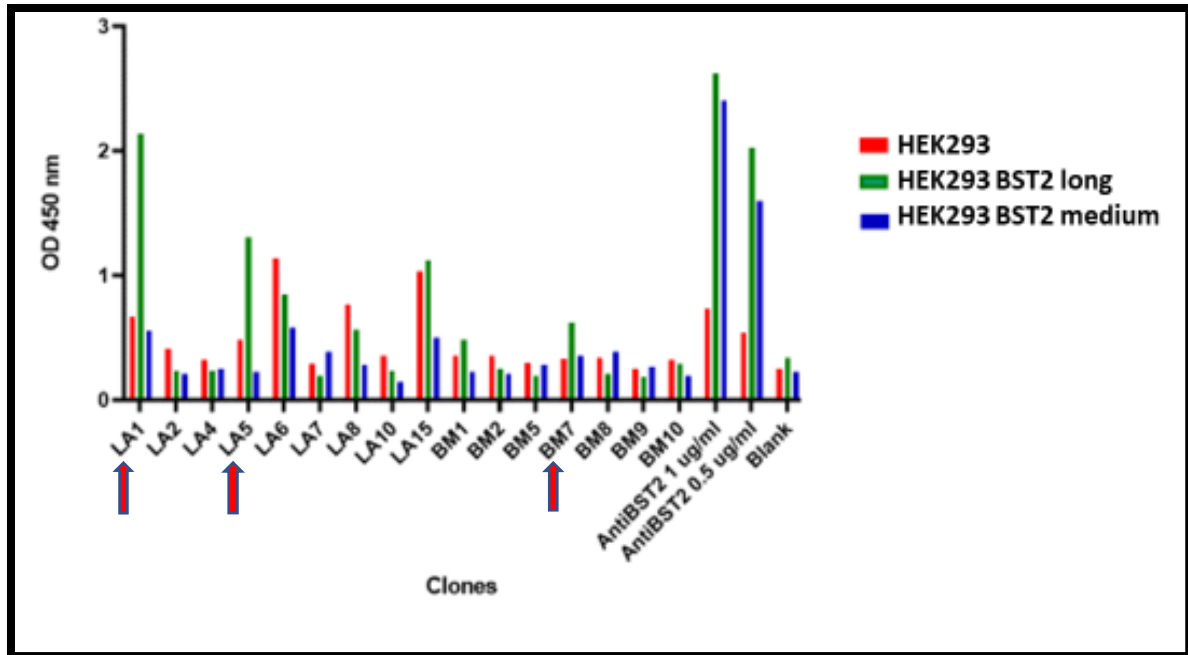


**Figure 3.4 Cell-based ELISA.**

Screening of selected supernatants occurred using HEK293 cell lines expressing different BST2 isoforms as indicated in the legend. Three clones (LA1, LA5 and BM7) were selected (marked with red arrows) based on specified criteria: high OD 450 signals with HEK293/BST2 long transfectants AND low signals with HEK293/BST2 medium and HEK293 parental cell lines.

### 3.4 Flowcytometry Staining of HEK293 Cell Lines

To confirm the results of the cell-based ELISA, staining of the HEK293 transfectants was examined by flow cytometry, using previously collected supernatants. Three clones (LA1, LA5 and BM7) generated the highest staining of HEK293-long cells that express the long isoform of BST2 and a weaker (or no) staining of the parental HEK293 and HEK293-medium cell lines(Figure 3.5).

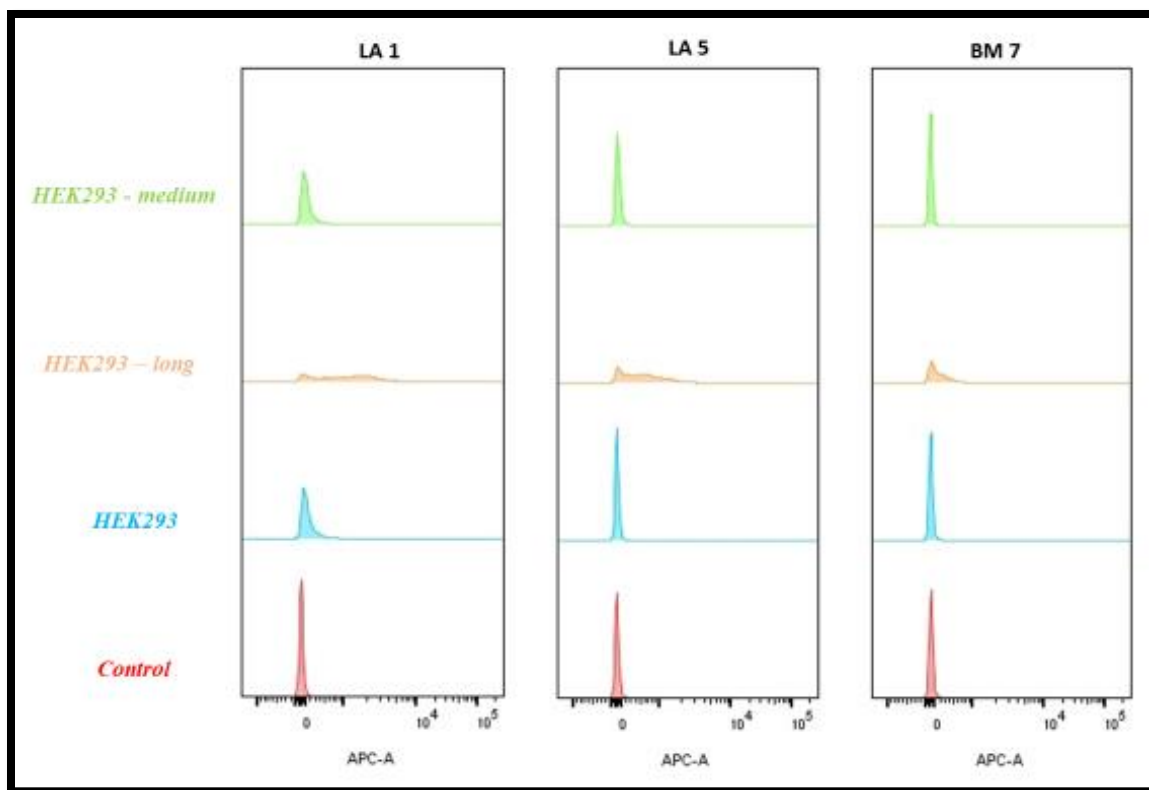


**Figure 3.5 Flowcytometry staining of the HEK293 cell lines.**

Using supernatants collected from the three selected clones (LA1, LA5, and BM7), the data showed maximum mean fluorescence staining of the HEK293-long transfectant and minimum staining of the other cell lines. For the control, only a secondary antibody (donkey anti-mouse APC conjugated) was used.

Flowcytometry analysis revealed that LA1 supernatant stained 70.9% of HEK293-long cells, with minimal staining of HEK293-medium transfectant and the HEK293 cells (1.6 and 2.2%, respectively). Using supernatant from BM7 was associated with less staining of the HEK293-long cells (39.8%) and minimum staining of the HEK293-medium and HEK293 parental cells (0.04% and 0.24%,

respectively). Compared to BM7, the LA5 supernatant was associated with a better staining of HEK293-long, with a percentage of 58.3% and comparable results for the HEK293 – medium and the parental (0.05% and 0.1%, respectively). Based on these results, LA5 clone demonstrated the best ability to generate MAbs with high affinity to the long isoform of BST2, with minimum interaction to the other isoform. It was therefore selected for subcloning and purification to ensure the purity of the clone selected and the consistency of the MAbs secreted.

After the purification and production of the anti-BST2 long MAb (clone LA5), at a concentration of 1 mg/ml, flow cytometry staining was repeated with the purified LA5 MAb and compared with the commercially available anti-BST2 (clone 26F8) MAb (Figure 3.6). The results from FACS staining confirmed the ability of the generated MAb to bind selectively to the transfectant expressing the long isoform of BST2 and not the medium isoform (49.8% and 0.28%, respectively). The results also demonstrated the differences between the generated clones LA5 and 26F8 MAbs, in terms of binding to the medium isoform of BST2 (0.28% and 96.7%, respectively).

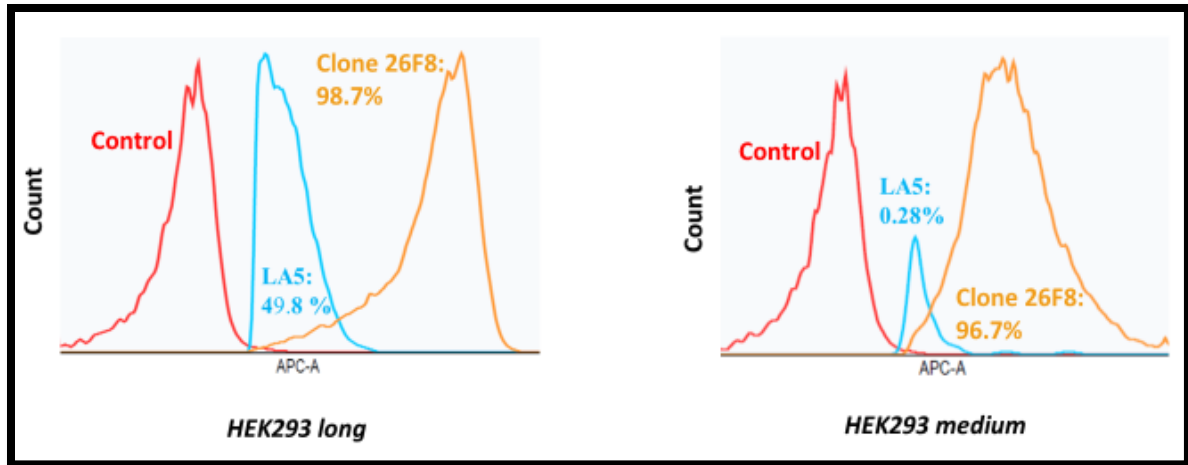


**Figure 3.6. Comparison between clones LA5 and clone 26F8.**

Flow cytometry staining of HEK293 long and HEK293 medium transfectants, using 1ug/ml of clones (LA5) and anti-BST2 (26F8) MAbs. This figure demonstrates the specificity of the generated antibody (LA5) to selectively bind to the long isoform. In contrast, the 26F8 MAb recognized both isoforms. APC conjugated secondary antibody alone was used as controls.

Figure 3.7 summarizes the processes and various screenings that led to the production of purified and concentrated Anti-BST2 long (Clone LA5) MAb.

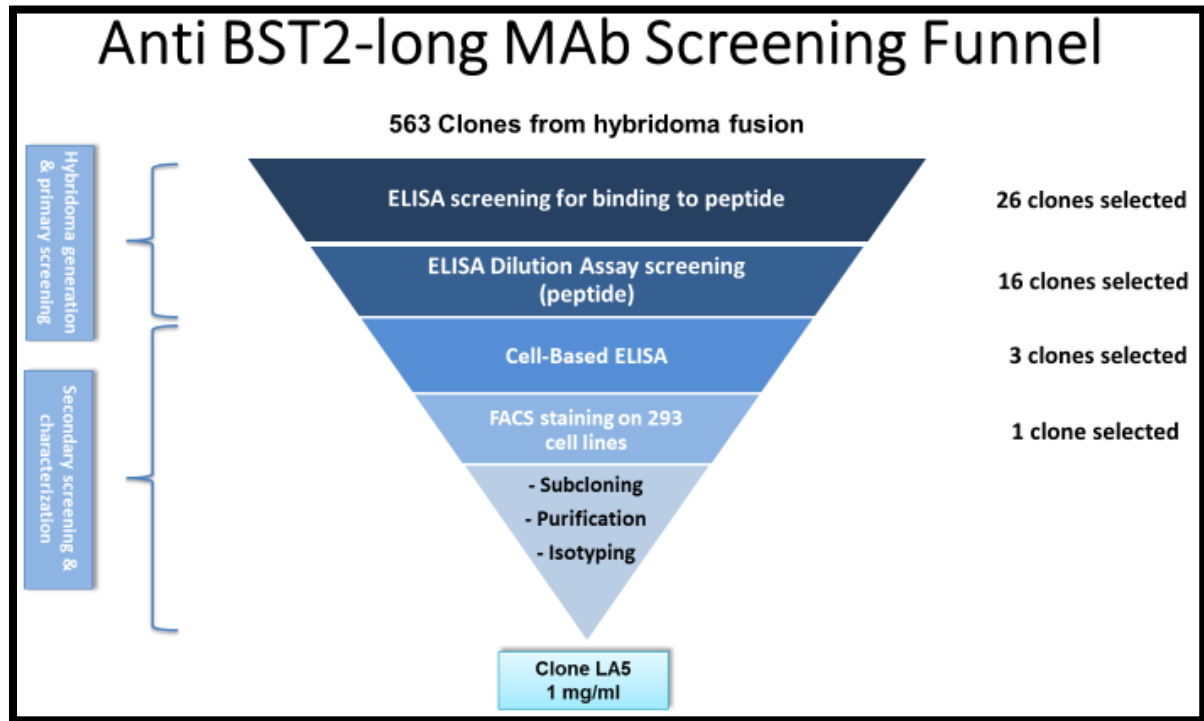


**Figure 3.7 Anti-BST2-long MAb Screening Funnel.**

The diagram shows the various screening steps performed after the generation of the hybridomas up to the selection of the MAb candidate, clone LA5, purified and concentrated.



### 3.5 Antibody Isotype

After subcloning and purification of the single clone (LA5), several experiments were performed on the anti-BST2-long MAb in order to define its characteristics. Using ELISA technique, isotype testing revealed the highest OD 450 signal with IgG1. The test was negative for IgM (non-significant low reactivity shown), IgG2a, IgG2b, IgG3 and IgA (Figure 3.8). Given these results, IgG1 isotype, commercially available clone was selected as the isotype control for all the experiments.

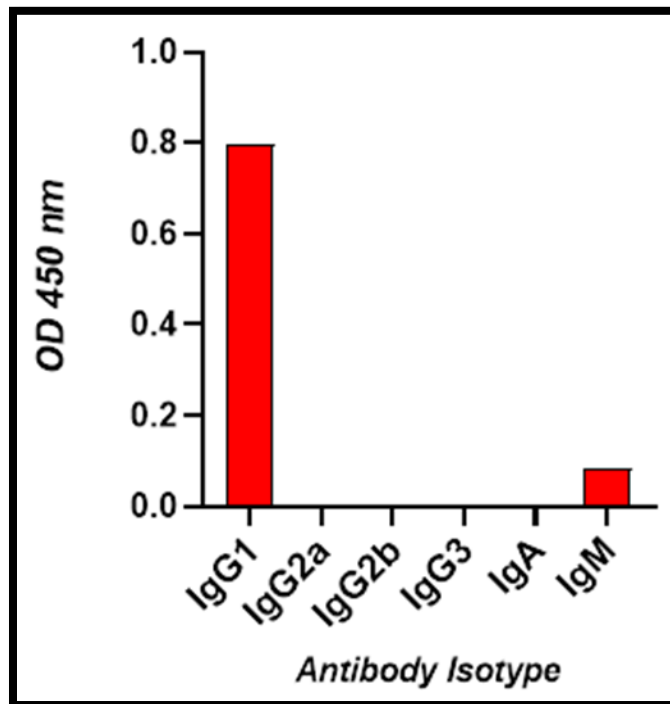


**Figure 3.8 Isotype ELISA test.** Isotype of clone LA5 was determined by an ELISA kit, following manufacturer recommendations.

### 3.6 Antibody Affinity

The binding kinetics of the anti-BST2-long MAb (clone LA5) was assessed, using Octet RED384 platform system. Briefly, antibodies were captured, as described under methods, by specific biosensors that bind the Fc region of the antibody. Based on multiple experiments and the standard operations procedures in our laboratory, a global fit of the data ( $R^2 = 0.9902$ ) revealed an association rate constant ( $K_a$ ) of  $2.0 \pm 0.019 \times 10^5 \text{ 1/Ms}$  and a dissociation rate constant ( $K_{dis}$ ) of  $9.21 \pm 0.12 \times 10^{-4} \text{ 1/s}$ . The calculated equilibrium dissociation constant ( $K_D$ ) of the LA5 MAb was  $4.61 \pm 0.074 \times 10^{-9} \text{ M}$ , a nanomolar value (Figure 3.9).

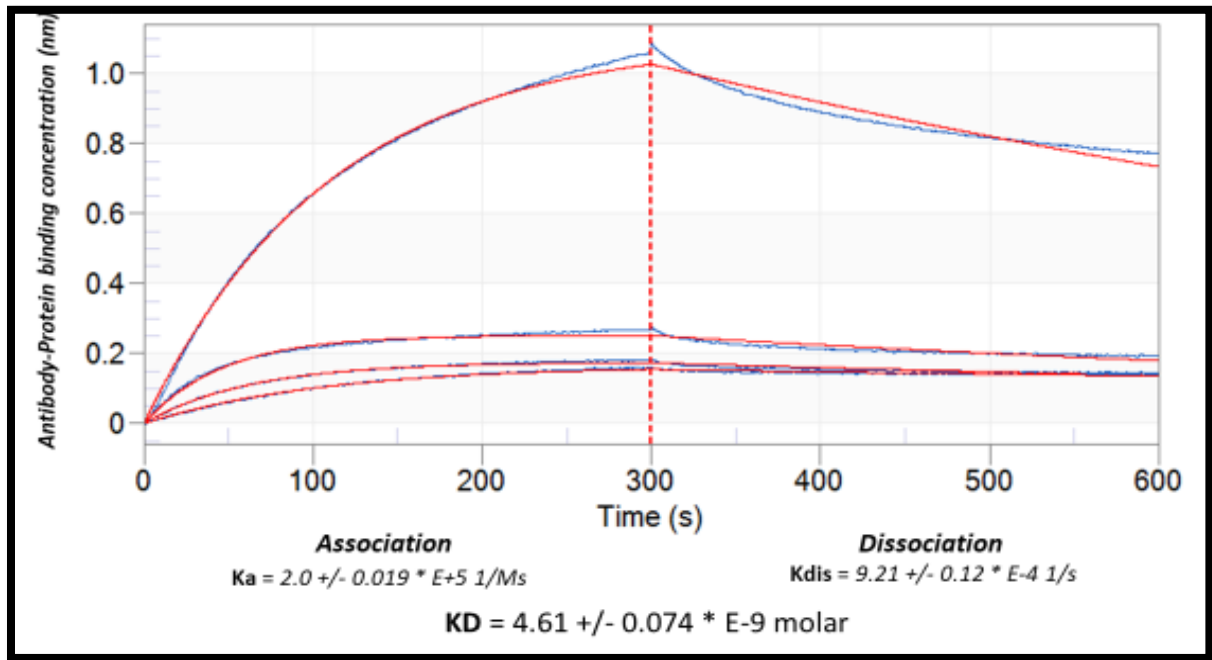


**Figure 3.9 Determination of  $K_a$ ,  $K_{dis}$  and  $K_D$  for LA5-antigen binding.**

The binding kinetics of anti-BST2-long clone LA5 (5 ug/ml) and BST2 protein at various concentrations (blue lines). The 1:1 fitting model is shown (red line).

Comparing the kinetics of both anti-BST2 clone 26F8 MAb and LA5, a difference of one order of magnitude was observed, indicating that our new generated antibody exhibits a better affinity (in the nanomolar range) than the previously generated 26F8 MAb. With a 1:1 binding model and a global fit of the data ( $R^2 = 0.9883$ ), the association rate constant ( $K_a$ ) was  $3.86 \pm 0.058 \times 10^4$  1/Ms and the dissociation rate constant ( $K_{dis}$ ) was  $1.32 \pm 0.019 \times 10^{-3}$  1/s. The calculated  $K_D$  of clone 26Fb was  $3.42 \pm 0.072 \times 10^{-8}$  molar (Figure 3.10).

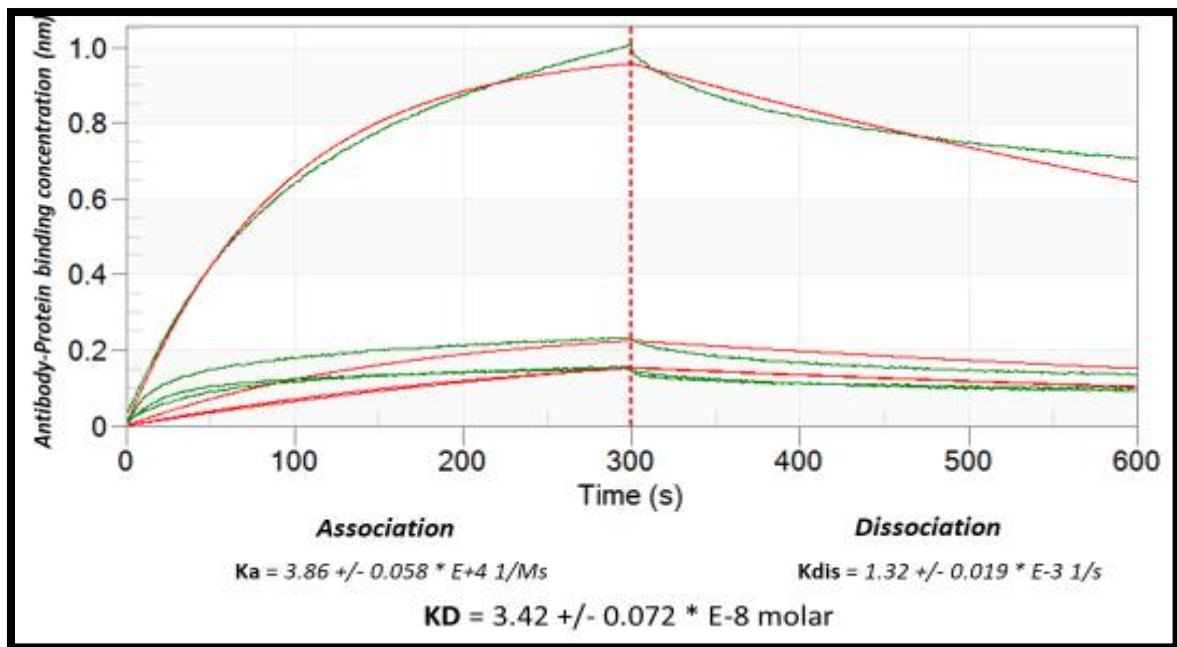


**Figure 3.10 Determination of  $K_a$ ,  $K_{dis}$  and  $K_D$  for 26F8-antigen binding.**

The binding kinetics of anti-BST2 clone 26F8 (5 ug/ml) and BST2 protein at various concentrations (green lines). The 1:1 fitting model is shown (red lines).

### 3.7 Antibody Specificity

As part of the characterization of the selected clone (LA5), we analyzed the antibody specificity using the approach of flow cytometry staining of MM1, a multiple myeloma cell line that constitutively expresses BST2. Staining of MM1 was assessed at different conditions, by directly incubating MM1 with LA5 or blocking the antibody binding to the cells through preincubation with recombinant BST2 protein, that contains the epitope used to generate the antibody. Appropriate negative control was performed by using an irrelevant protein for blocking. Anti-BST2-long (clone LA5) was pre-incubated with BST2 protein for 10 minutes, before being transferred to the U-bottom wells containing MM1 cells. Using the BST2 protein-preincubated MAb, the staining percentage of the MM1 cells was reduced from 85.2% to 5.01% (Figure 3.10). This significant reduction suggested the strong specific binding of the MAb to the BST2 protein, leaving less free MAb available for binding to the BST2 receptors on the MM1 cells. Alternatively, Spartan protein, or SprT-like domain-containing protein, a human DNA-binding metalloprotease with 489 amino acid length and involved in the response to DNA replication errors (34, 35) was used as an irrelevant protein. Preincubating LA5 MAb with this protein for 10 minutes did not change the percentage of staining, compared with the direct incubation of the MAb with MM1 cells (85.2% and 83.9%, respectively) (Figure 3.11). The same pattern was observed with the use of anti-BST2 (26F8) MAb; the percentage of stained cells with 26F8 MAb was 98.2%, 2.6% when preincubated with recombinant BST2, and 98.1% when preincubated with Spartan protein (Figure 3.12). These results accurately indicated the ability of the generated MAb to bind specifically to the BST2

receptors expressed on the surface of MM1 and demonstrate the comparability of the generated antibody to the commercially available anti-BST2 26F8 MAb, in terms of specificity (Figure 3.13).

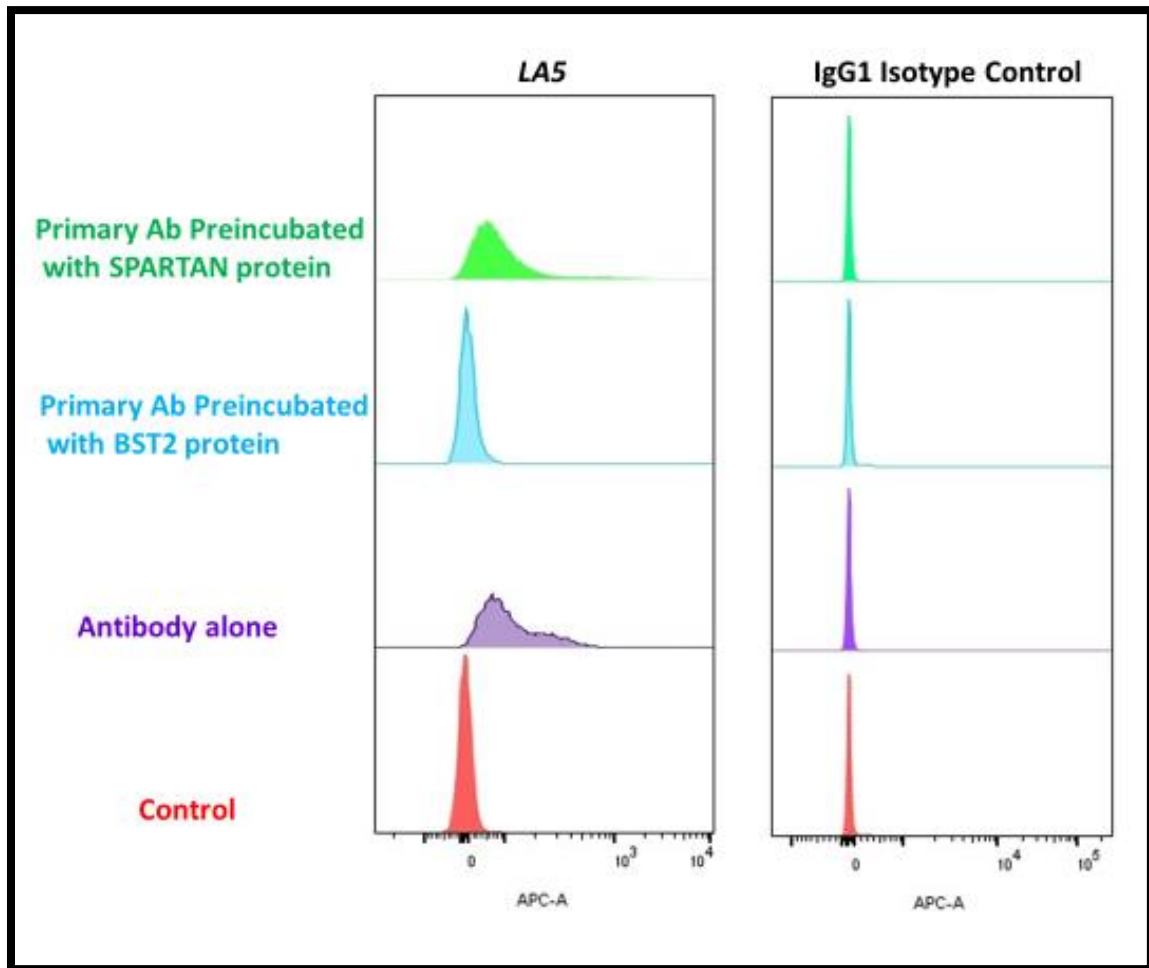


**Figure 3.11 LA5 MAb specificity.**

Flowcytometry staining of MM1 cell line, using the generated MAb LA5 and IgG1 isotype control. The percentage of cell staining was reduced from 85.2% to 5.01% when LA5 MAb was preincubated with BST2 protein (5 ug/ml), while preincubation with Spartan protein did not lead to this reduction. In both columns, secondary antibody (donkey anti-mouse APC-conjugated) was used alone as a control.

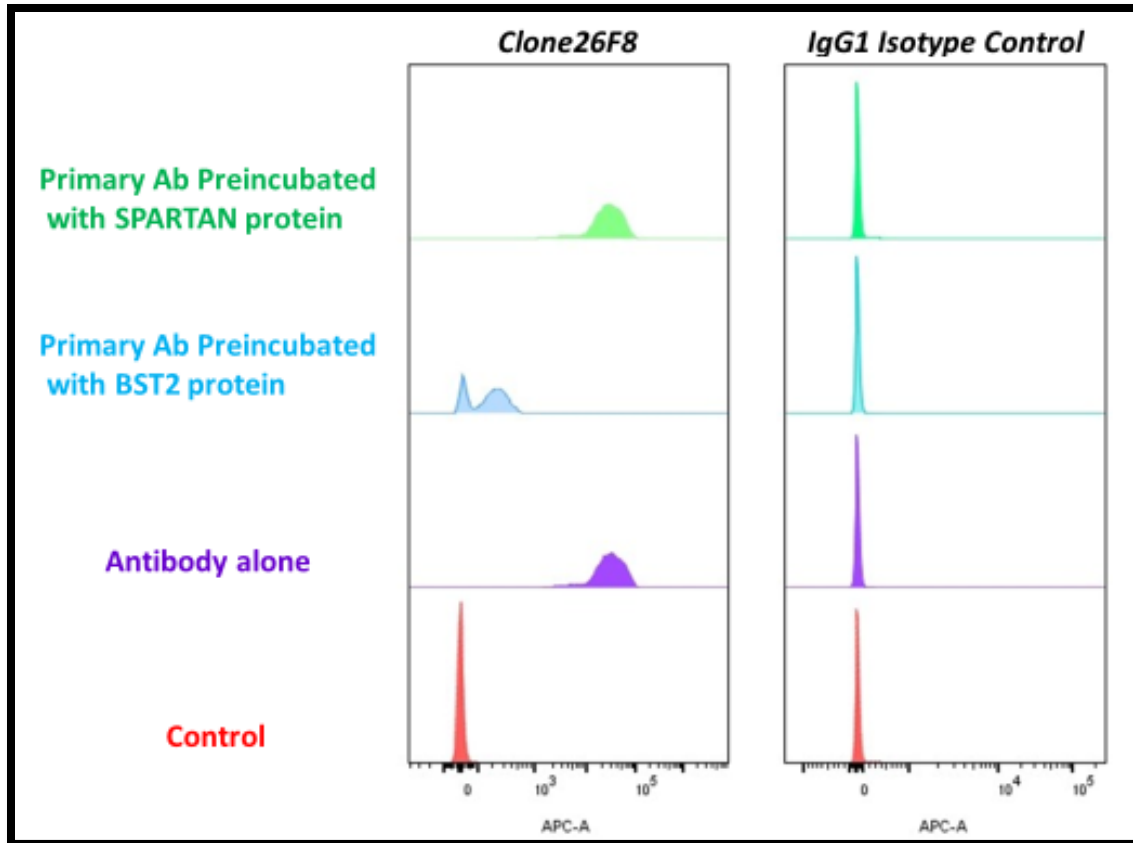


**Figure 3.12 26F8 MAb specificity.**

Flowcytometry staining of MM1 cell line using anti-BST2 (clone 26F8) MAb and IgG1 isotype control. The percentage of cell staining was reduced from 98.2% to 2.6% when the 26F8 MAb was preincubated with BST2 protein, while preincubation with Spartan protein was not associated with a reduction. In both columns, secondary antibody (Donkey anti-mouse APC-conjugated) was used alone as a control.

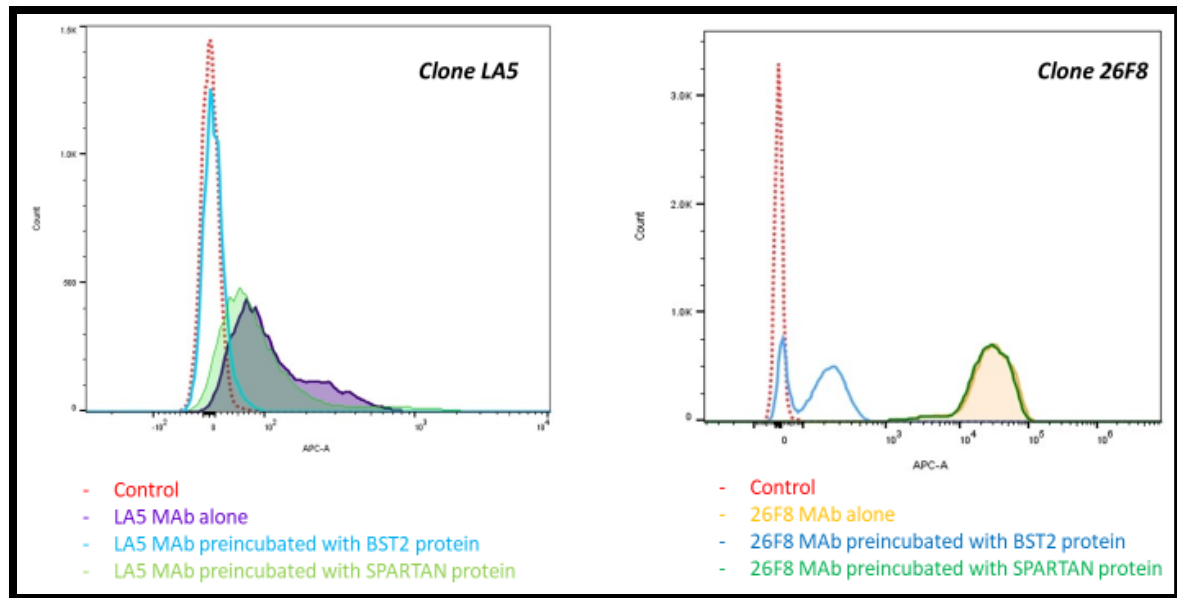


**Figure 3.13 Specificity comparison of the LA5 and 26F8.**

Flowcytometry staining of MM1 cell line using of the generated anti-BST2-long (clone LA5) MAb and anti-BST2 (clone 26F8) MAb, preincubated with recombinant BST2 protein or irrelevant protein and using secondary antibody alone as a control. This figure demonstrates the comparability between these two MAbs, in terms of specificity.

### **3.8 Flow Cytometry Staining of B Lineage and Breast Tissue Cell Lines**

To analyze the expression of the long BST2 isoform in cancer and normal tissues, and to test our hypothesis that the long isoform is preferentially expressed in tumor tissues, the generated MAb (anti-BST2-long clone LA5) was used in FACS staining of two sets of cell lines, representing normal and malignant plasma cells and breast tissue. Observing differences in the cell staining percentages and intensity (mean fluorescence) between the normal and malignant cell lines might indicate a preferential expression of the long isoform of BST2 receptor. Using B lymphoblastoid cell lines (B-LCL) as a surrogate for normal B lymphocytes, no differences were observed in the cell staining percentage or mean fluorescence, when compared to MM1 and U266 multiple myeloma cell lines. Using LA5 MAb, the percentage of cell staining for B-LCL, MM1 and U266 were 99.3, 98.6, and 96.1%, respectively. This pattern of staining was also noticed with anti-BST2 26F8 MAb that recognizes both isoforms. No significant differences were observed and the percentage of cell staining for B-LCL, MM1 and U266 were 99.7, 99.6, and 97.1%, respectively (Figure 3.14). While the FACS results clearly confirmed the expression of the long BST2 isoform on the malignant B cells, it did not prove the preferential expression in malignant vs non-malignant B cell lineages. These results might suggest a non-specific expression of the long isoform of BST2 in the spectrum of B cells. The mean fluorescence of cell staining with anti-BST2-long (clone LA5) or anti-BST2 (clone 26F8) MAbs in B-LCL and U266 was similar, suggesting that the long isoform is not restricted to malignant cells but is also present in normal cells (B-LCL) (Figure 3.14).



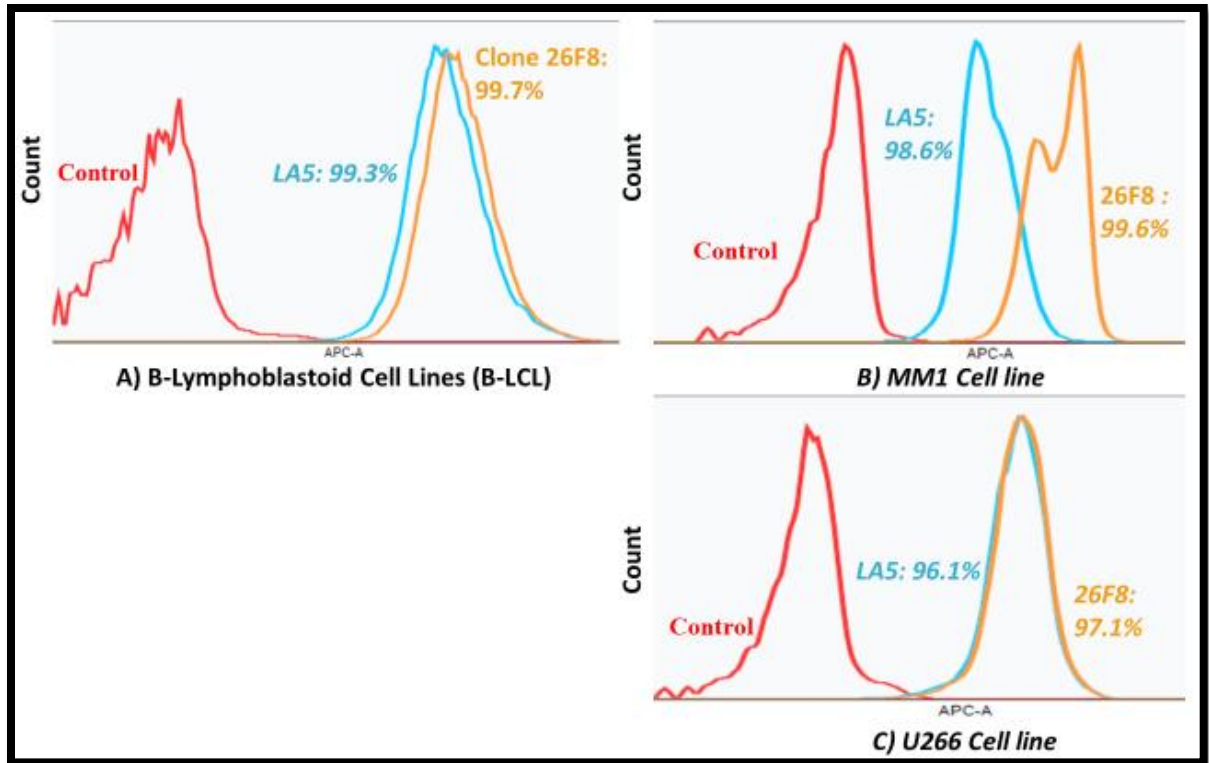


**Figure 3.14 Flow cytometry staining of B cell lines.**

FACS staining of three cell lines, representing normal and malignant plasma cells, using the generated MAb against the long isoform of BST2 (LA5), and Anti-BST2 (26F8), at a concentration of 1ug/ml. The secondary antibody alone was used as a control.

- A. B-LCL cell line. No statistically significant differences in staining were observed with the use of LA5 or 26F8 MAbs. The percentage of cell staining was 99.3% and 99.7%, respectively. Since 26F8 recognizes both isoforms, and LA5 only the long isoform, it could be assumed that only the long isoform is expressed.
- B. MM1 cell line. No statistically significant differences in staining were observed with the use of LA5 or 26F8 MAbs. The percentage of cell staining was 98.6%

and 99.6%, respectively. The mean fluorescence was different, suggesting different molecule density on the cell surface.

C. U266 cell line. No statistically significant differences in staining were observed with the use of LA5 or 26F8 MAbs. The percentage of cell staining was 96.1% and 97.1%, respectively, suggesting that only the long isoform is expressed.

In contrast to the B cell lines, FACS staining of breast tissue cell lines demonstrated different patterns with these two MAbs. At a concentration of 1 ug/ml, LA5 MAb showed minimal binding to MCF-10A, a non-malignant epithelial breast tissue cell line, as well as T47D, MDA-MB-231 and MCF7 human breast cancer cell lines. Percentages of cell staining were 2.4%, 2.6%, 1% and 0.43%, respectively (Figure 3.15). Using this same concentration, anti-BST2 clone 26F8 MAb resulted in a significantly higher staining of the MCF-10A cell line (staining percentage of 27.7% and p value < 0.05). Staining of the human breast cancer cell lines varied; upon comparison to the intensity of MCF-10A staining, insignificant differences were observed with MDA-MB-231 and MCF7 (percentage of staining was 28.4% and 34.7%, respectively). However, a significant difference was noticed with the staining of the T47D human breast cancer cell line, with percentage of cell staining of 96.6% (Figure 3.15). With these results, neither MAbs revealed the differential expression of BST2 isoforms in the malignant versus nonmalignant cell lines, using flow cytometry staining.

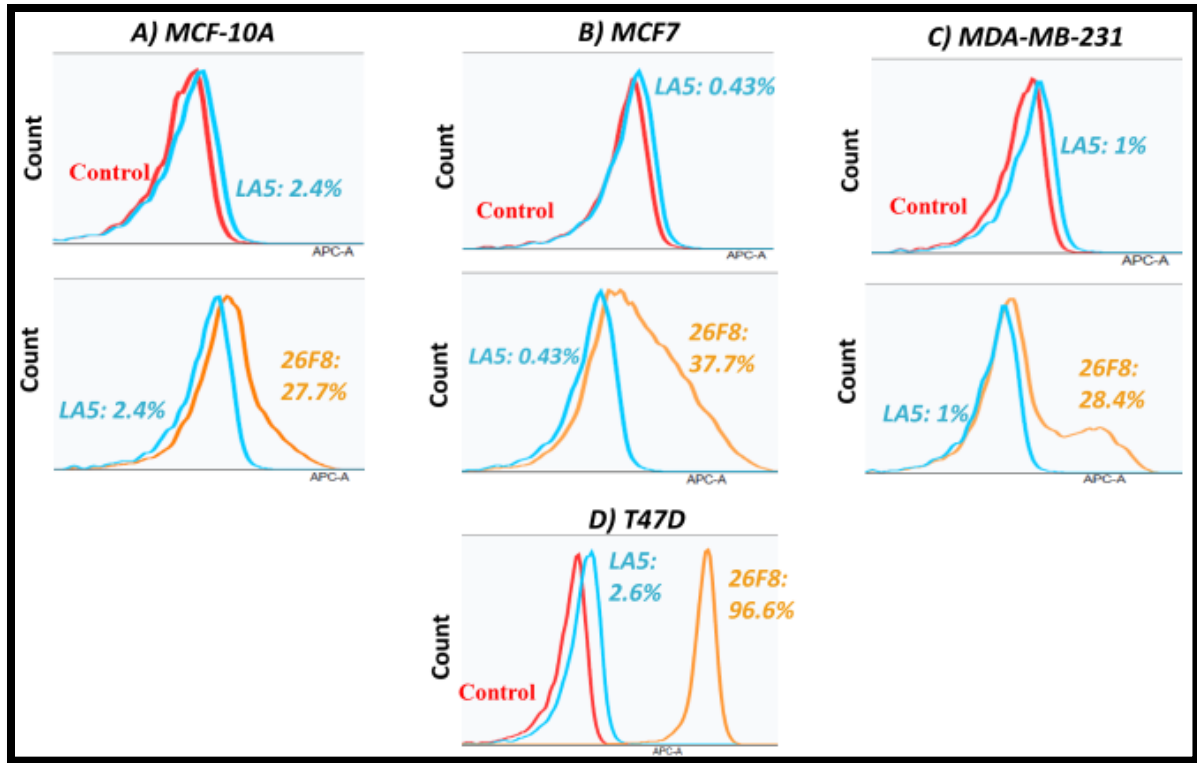


**Figure 3.15 Flow cytometry staining of breast tissue cell lines.**

FACS staining of four cell lines, representing normal and malignant breast tissue cells, using the MAb against the long isoform of BST2 (clone LA5) and the Anti-BST2 (clone 26F8). Secondary antibody APC conjugated was used alone as a control.

- A. MCF-10A cell line: statistically significant differences ( $p$  value  $< 0.05$ ) in staining were observed with the use of LA5 or 26F8 MAbs. The percentage of cell staining was 2.4% and 27.7%, respectively.
- B. MCF7 cell line: statistically significant differences ( $p$  value  $< 0.05$ ) in staining were observed with the use of LA5 or 26F8 MAbs. The percentage of cell staining was 0.43% and 34.7%, respectively.

- C. MDA-MB-231 cell line: statistically significant differences ( $p$  value  $< 0.05$ ) in staining were observed with the use of LA5 or 26F8 MAbs. The percentage of cell staining was 1% and 28.4%, respectively.
- D. T47D cell line: statistically significant differences ( $p$  value  $< 0.05$ ) in staining were observed with the use of LA5 or 26F8 MAbs. The percentage of cell staining was 2.6% and 96.6%, respectively.

### **3.9 Immunohistochemistry Staining**

To examine the diagnostic potential of the generated MAb and to determine the localization of the long isoform of BST2, immunohistochemistry technique was selected. The immunohistochemistry assays on the HEK-293 transduced cells demonstrated the ability of LA5 MAb to stain cells expressing the long isoform of BST2, but not the other isoforms. In contrast, the use of the 26F8 MAb was associated with the staining of cells expressing either isoform of BST2 (Figure 3.16). Moreover, these antibodies resulted in membranous to cytoplasmic staining, suggesting the potential of the internalization of this isoform.

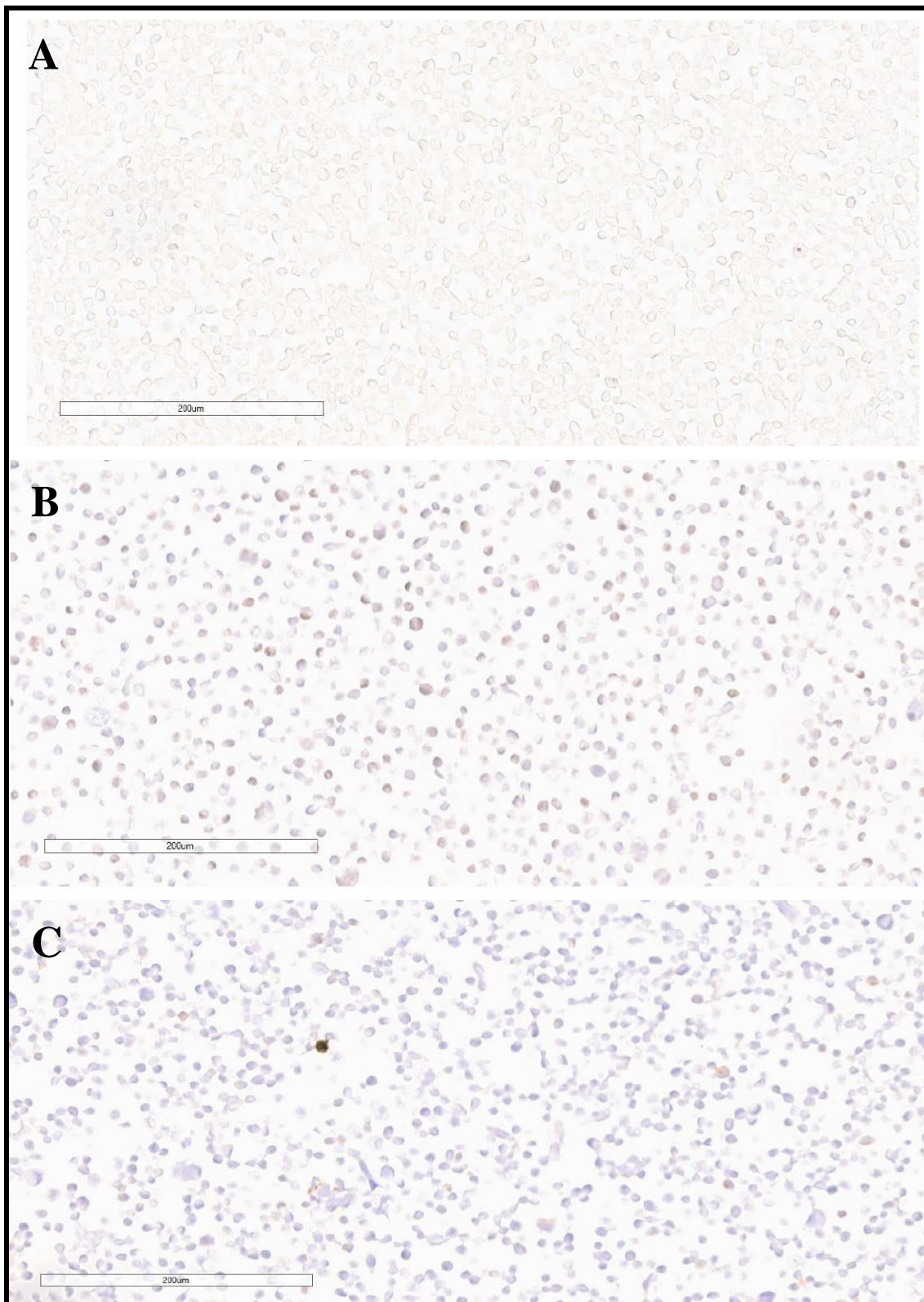


**Figure 3.16 Immunohistochemistry staining of HEK293 cell lines.**

The staining patterns of transduced HEK-293 cell lines, using anti-BST2-long (clone LA5) and anti-BST2 (clone 26F8) MAbs, are as follow:

- A. Negative control (no staining).
- B. With LA5 MAb, cells expressing the long isoform of BST2 demonstrated grainy membranous to cytoplasmic staining, while no staining was observed in cell expressing the medium isoform.
- C. Positive control using anti-BST2 (clone 26F8) MAb. Membranous to cytoplasmic staining was observed in HEK293 cells expressing both the long and medium isoforms of BST2.

Through collaboration with Dr. Bravo's laboratory at Hospital El Cruce (Buenos Aires, Argentina), immunohistochemistry staining was performed on patient-derived samples of breast cancer with these two antibodies. Using formalin fixed paraffin embedded (FFPE) tissue blocks of ductal breast carcinoma, the generated anti-BST2-long MAb (LA5) was able to stain and identify infiltrating carcinoma cells, but not the normal surrounding acinar cells. In contrast, the anti-BST2 clone 26F8 MAb stained cells expressed BST2 but did not discriminate between the malignant cells and the surrounding normal acinar cells (Figure 3.17).



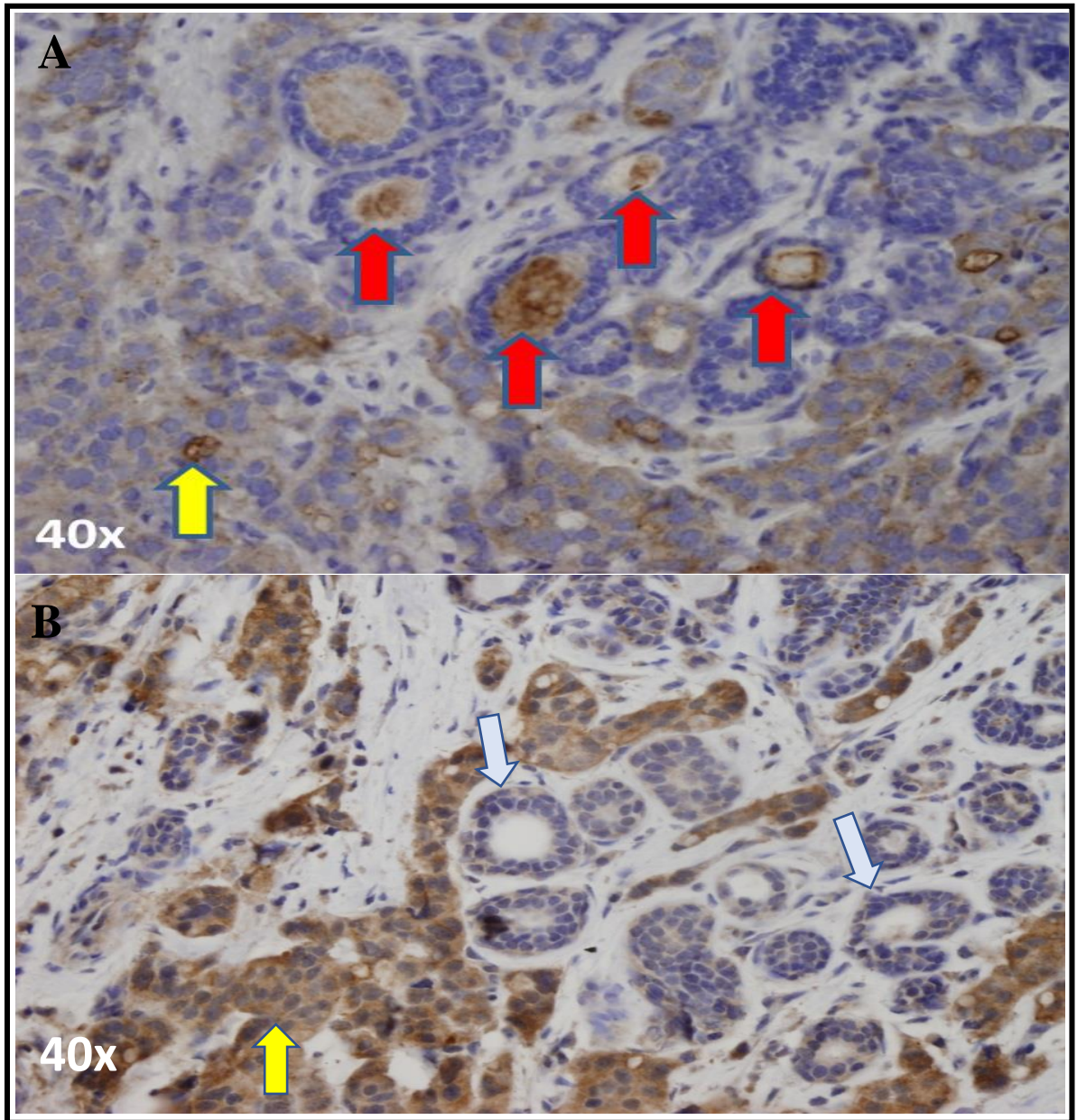


**Figure 3.17 Immunohistochemistry slides of infiltrating ductal breast carcinoma surrounding normal acinus (Slides credit: Dr. Ines Bravo).**

Immunohistochemistry staining of breast cancer tissue revealing the expression of the long isoform of BST2 protein.

- A. Infiltrating ductal breast carcinoma (yellow arrow) surrounding normal acinus (red arrows), using anti-BST2 clone 26F8 MAb. This antibody stained both the normal and malignant cells.
- B. Infiltrating ductal breast carcinoma (yellow arrow) surrounding normal acinus (white arrows), using anti-BST2-long clone LA5 MAb. This antibody stained the malignant cells only.

Within the breast ductal system, immunohistochemistry assays revealed the ability of the LA5 MAb to bind and stain specifically the malignant cells and to distinguish the surrounding normal ducts. On the other hand, the 26F8 MAb could not differentiate between the normal and malignant ducts, with a subsequent positive staining of cells in these two structures (Figure 3.18). This finding suggested that the specific epitope of LA5 that present in the long BST2 isoform might be exposed with tissue fixation and processing, thus allowing LA5 to recognize tumor cells specifically.



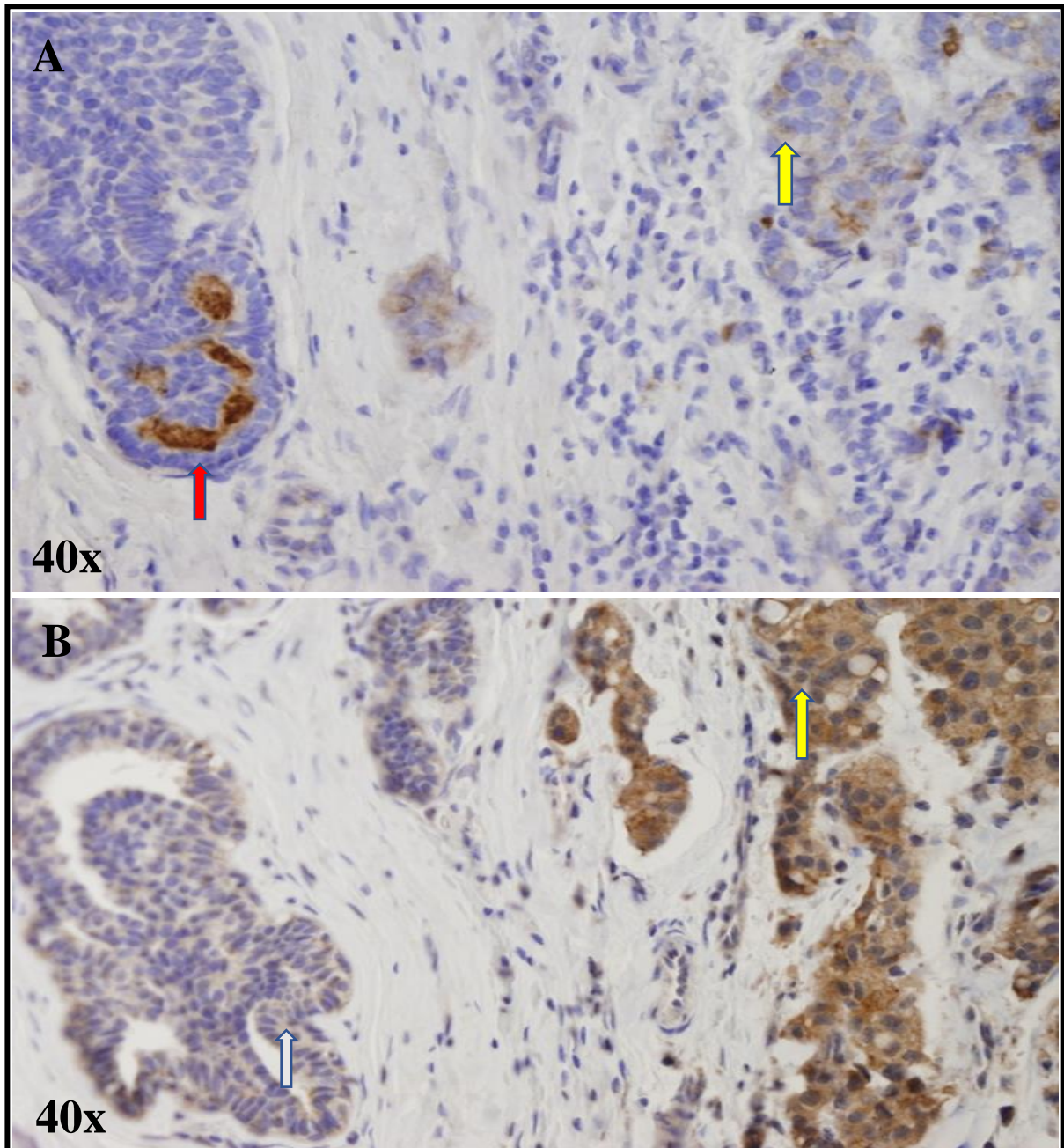


**Figure 3.18 Immunohistochemistry slides of infiltrating ductal breast carcinoma surrounding normal ducts (Slides credit: Dr. Ines Bravo).**

Immunohistochemistry staining of breast cancer tissue reveals the expression of the long isoform of BST2 protein in malignant cells.

- A. Infiltrating ductal breast carcinoma (yellow arrow) surrounding normal ducts (red arrow), using anti-BST2 clone 26F8 MAb. This antibody stained both the normal and malignant cells.
- B. Infiltrating ductal breast carcinoma (yellow arrow) surrounding normal ducts (white arrow), using anti-BST2-long clone LA5 MAb. This antibody stained the malignant cells only.

### **3.10 BST2 Silencing Via shRNA**

To explore BST2 roles in breast tissue carcinogenesis, a loss of function approach with BST2-targeting short hairpin RNA (shRNA) was used. To examine the efficiency of this approach, flowcytometry staining of cell lines was performed. By analyzing the percentage of cell staining among the non-transduced T47D cell line (T47D-WT), T47D cell line with a non-silenced transduction (T47D-NS), and T47D cell line with BST2-silenced transduction (T47D BST2-silenced), I was able to confirm a subpopulation of cells that were GFP-positive and APC-negative. The green fluorescent protein (GFP) indicates efficient lentiviral transduction, while APC-conjugated secondary antibodies that interact with anti-BST2 primary antibodies suggests the presence of BST2 membrane receptors (Figure 3.19). Consequently, the GFP-positive APC-negative cells were considered BST2-silenced cells. Those cells were collected via cell sorting, expanded, and studied in comparison to T47D-WT (GFP-negative, APC-positive cells) and T47D NS (GFP-positive, APC-positive cells).

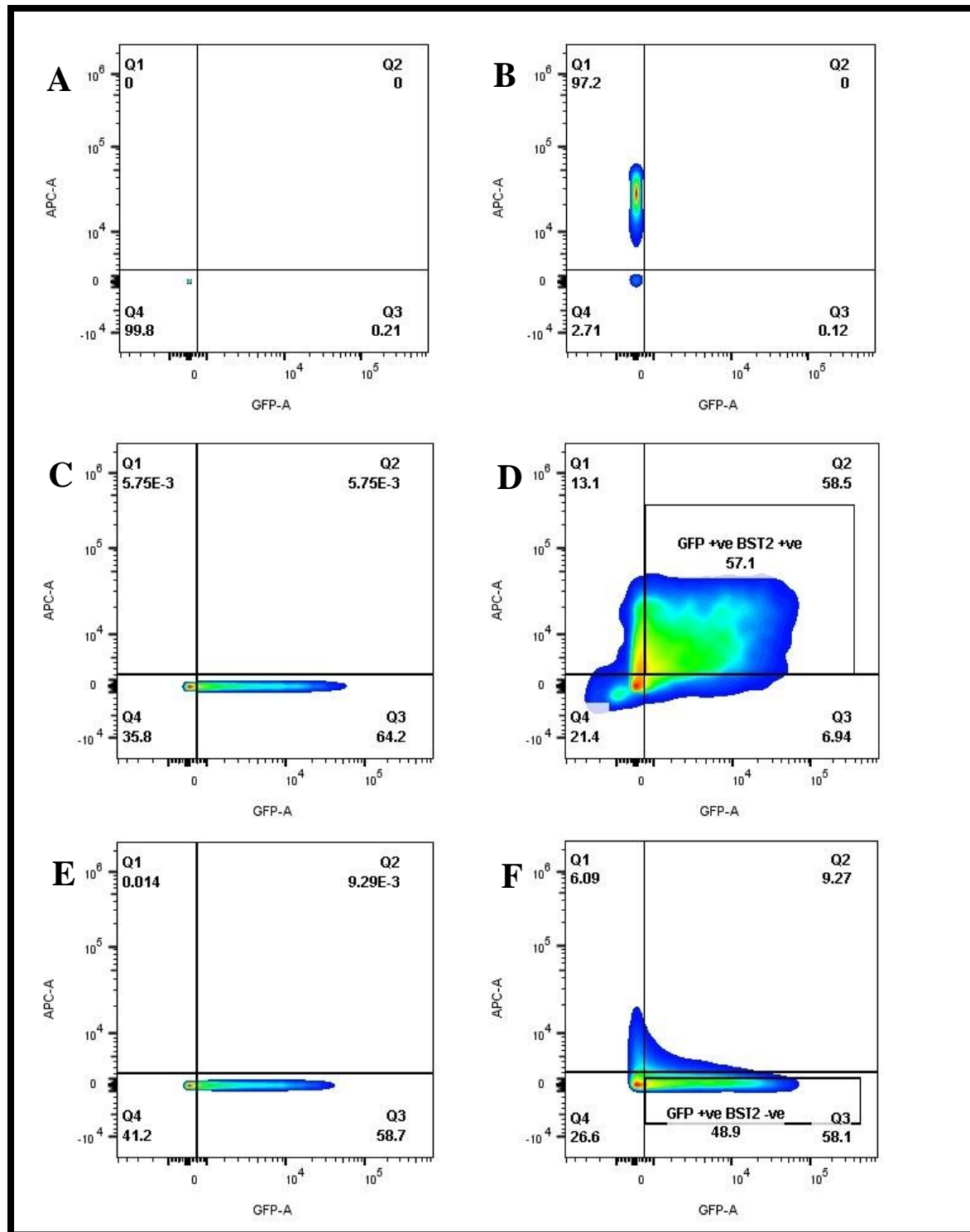


Figure 3.19 Flow cytometry dot plots of T47D cell lines.

A and B: Dot plot figures of **T47D-WT** staining, using APC-conjugated secondary antibodies alone as a control (Figure A) and anti-BST2 clone 26F8 in a concentration of 2 ug/ml and secondary antibodies conjugated with APC (Figure B).

C and D: Dot plot figures of **T47D-NS** staining, using APC-conjugated secondary antibodies alone as a control (Figure C) and anti-BST2 clone 26F8 in a concentration of 2ug/ml and secondary antibodies conjugated with APC (Figure D).

Figure C shows a population of cells (64.2%) that is GFP-positive, while figure D demonstrates a percentage of GFP +ve, APC +ve cells = 57.1%. These GFP +ve, BST2 +ve cells were collected via cell sorting, and considered a T47D cell line with a nonsilenced transduction (T47D-NS).

E and F: Dot plot figures of **T47D BST2-silenced** staining, using APC-conjugated secondary antibodies alone as a control (Figure E) and anti-BST2 clone 26F8 in a concentration of 2ug/ml and secondary antibodies conjugated with APC (Figure F).

Figure E shows a population of cells (58.7 %) that is GFP-positive, while Figure F demonstrates a percentage of GFP +ve, APC -ve cells = 48.9%. These GFP +ve, BST2 -ve cells were collected via cell sorting, and considered a T47D cell line with a BST2 silenced transduction (T47D BST2-silenced).

### 3.11 Cell Viability Assay

To examine the impact of BST2 silencing on the viability of T47D, CellTiter-Glo viability assay was performed. A statistically significant reduction in viability was observed with BST2 silencing ( $p$  value = 0.033), compared to the viability observed in T47D-WT and T47D-non silenced controls. Figure 3.20 demonstrates the mean and 95% confidence intervals of the luminescence captured from each cell line.

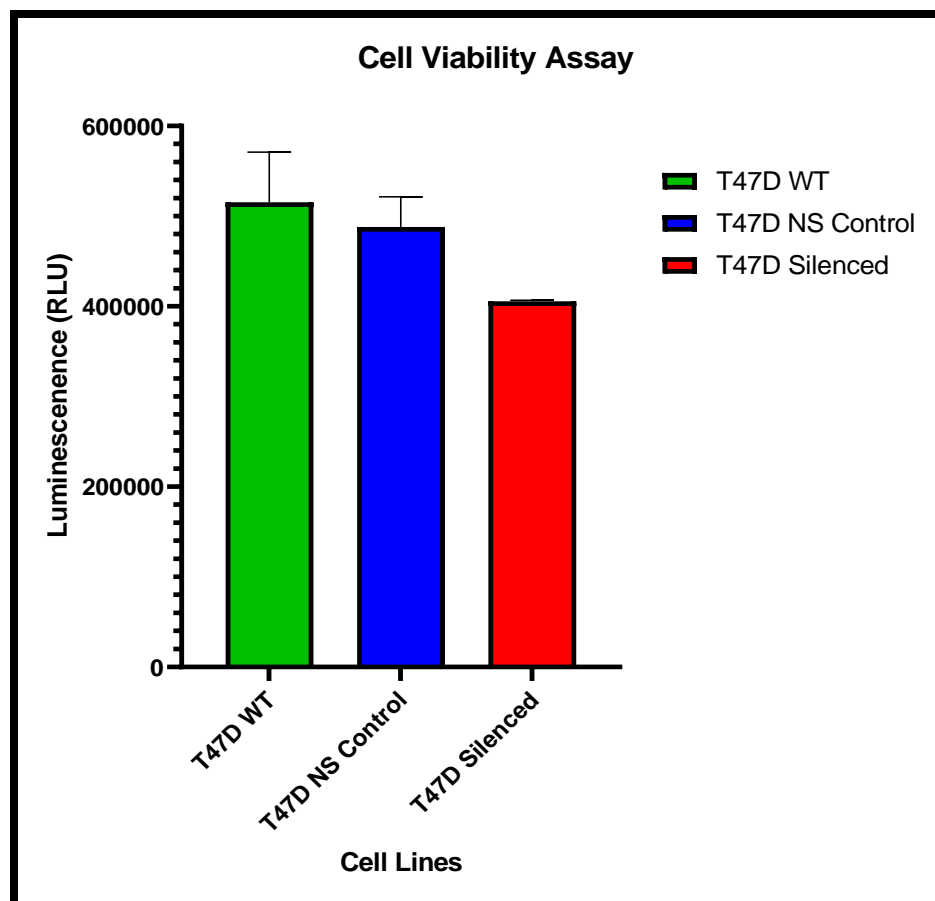


**Figure 3.20 Cell Viability assay.** This figure shows the statistically significant reduction in the viability of the T47D cell line with silenced BST2 ( $P < 0.05$ ), compared to T47D WT and nonsilenced T47D transfectant.

### 3.12 Cell Proliferation Assay

To examine the impact of BST2 silencing on the proliferation of T47D, XTT cell proliferation assay was performed. No statistically significant change was observed with BST2 silencing ( $p$  value = 0.6), compared to the proliferation observed in T47D-WT and T47D-non silenced controls. Figure 3.21 demonstrates the mean and 95% confidence intervals of the absorbance recorded from each cell line.

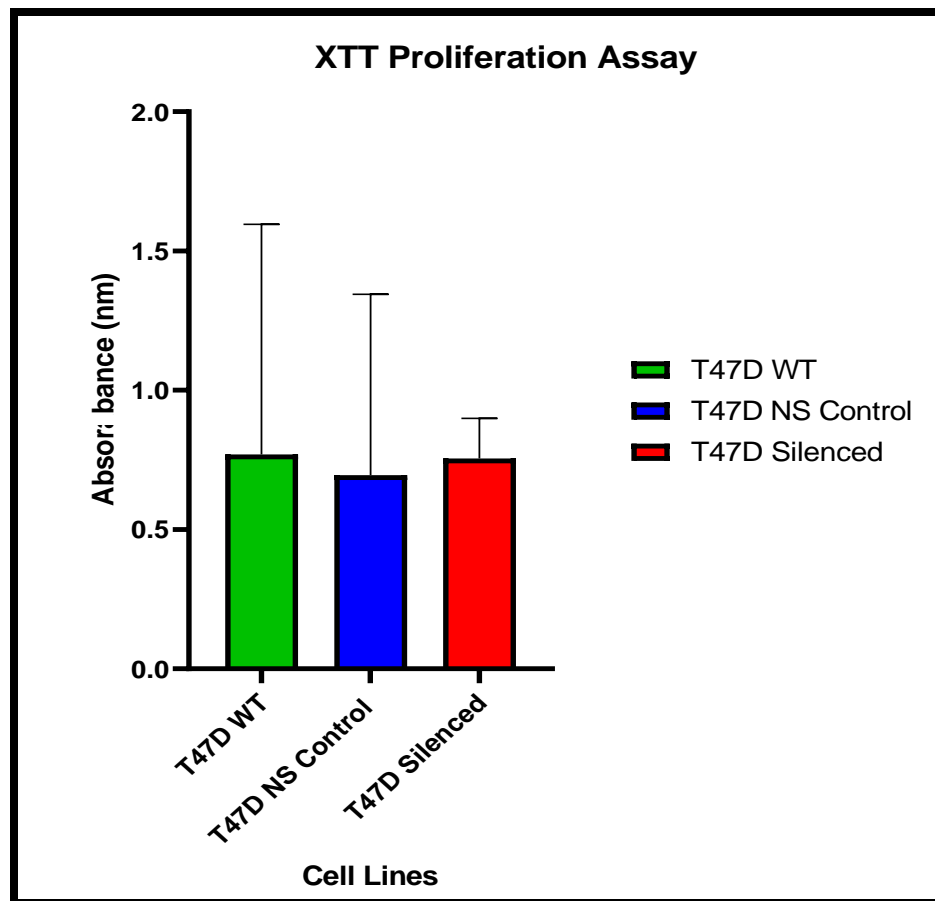


**Figure 3.21 Cell Proliferation assay.** This figure shows no statistically significant change in the proliferation of the T47D cell line with silenced BST2 ( $p$  value = 0.6), compared to T47D WT and nonsilenced T47D transfectant.

### **3.13 Protein Expression in T47D Cell Lines Pre- and Post BST2 Silencing**

To define the adaptive cellular responses to the silencing of BST2 gene and understand a possible pathway to reduced viability post-BST2 silencing, cellular protein expression was explored. The data received from the Reverse Phase Protein Array (RPPA) assessed the relative protein expression of 466 genes in a non-transduced T47D cell line (T47D-WT), T47D cell line with a nonsilenced transduction (T47D-NS), and T47D cell line with BST2 silenced transduction (T47D BST2-silenced). After data cleaning and value analysis, the relative protein expression of 99 genes showed changes after BST2 silencing. The log<sub>2</sub> values of the normalized linear data were median-centered and used to generate a heatmap to visualize the changes in the relative protein expression observed after BST2 silencing, compared to T47D-WT and T47D-NS (Figure 3.22).

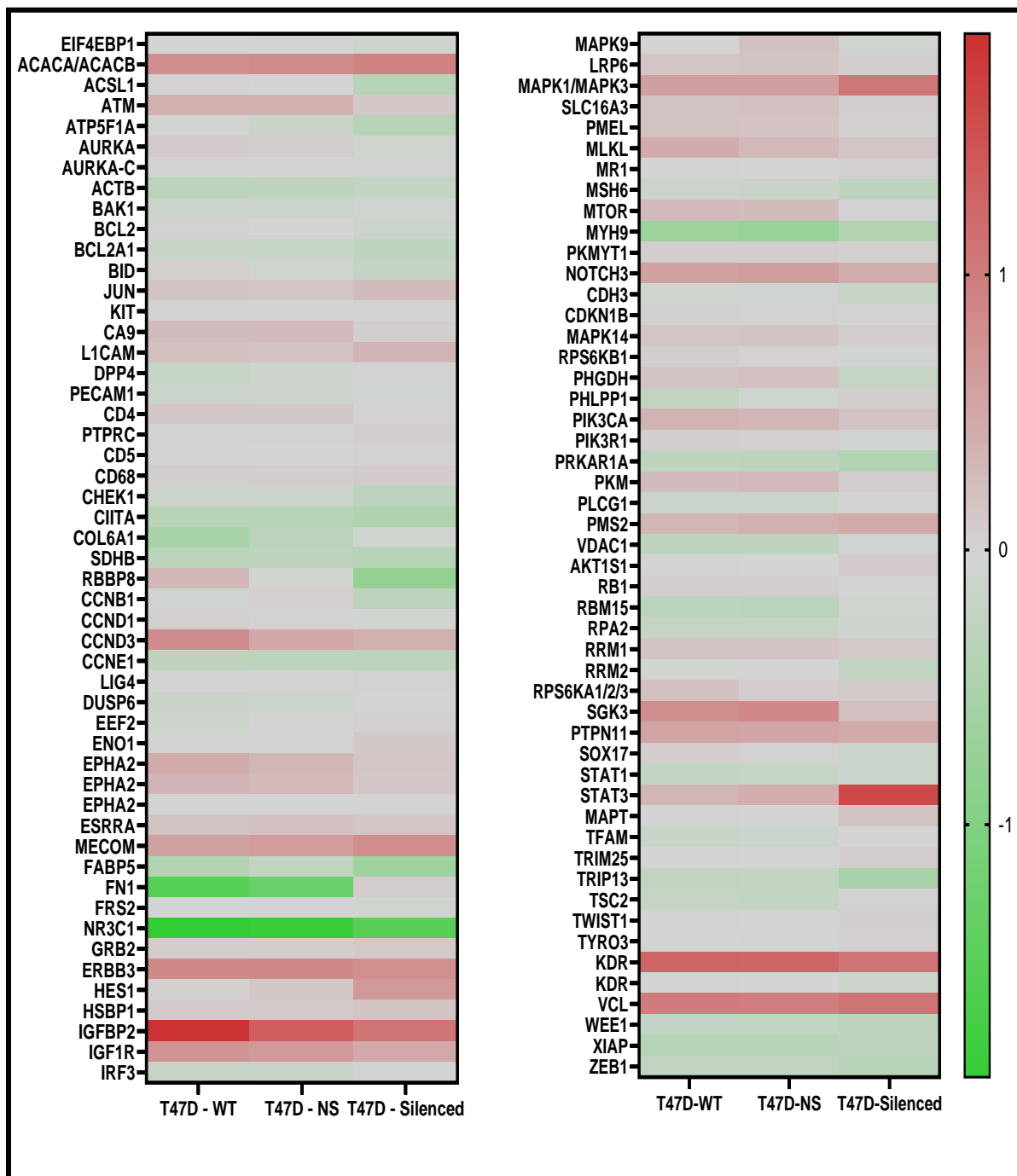


**Figure 3.22 Heatmap of T47D cell lines.**

This heatmap visualizes the changes in the protein expression of 99 genes associated with the silencing of the BST2 gene in T47D cell lines. The red color



suggests an increase above the median value, while the green color suggests a decrease below the median value.

By analyzing the normalized linear values associated with each protein, statistically significant upregulation ( $p$  value  $< 0.05$ ) was found in the following genes with the silencing of BST2: MAPK1/MAPK3, HES1, FN1 and STAT3 (Figure 3.23).

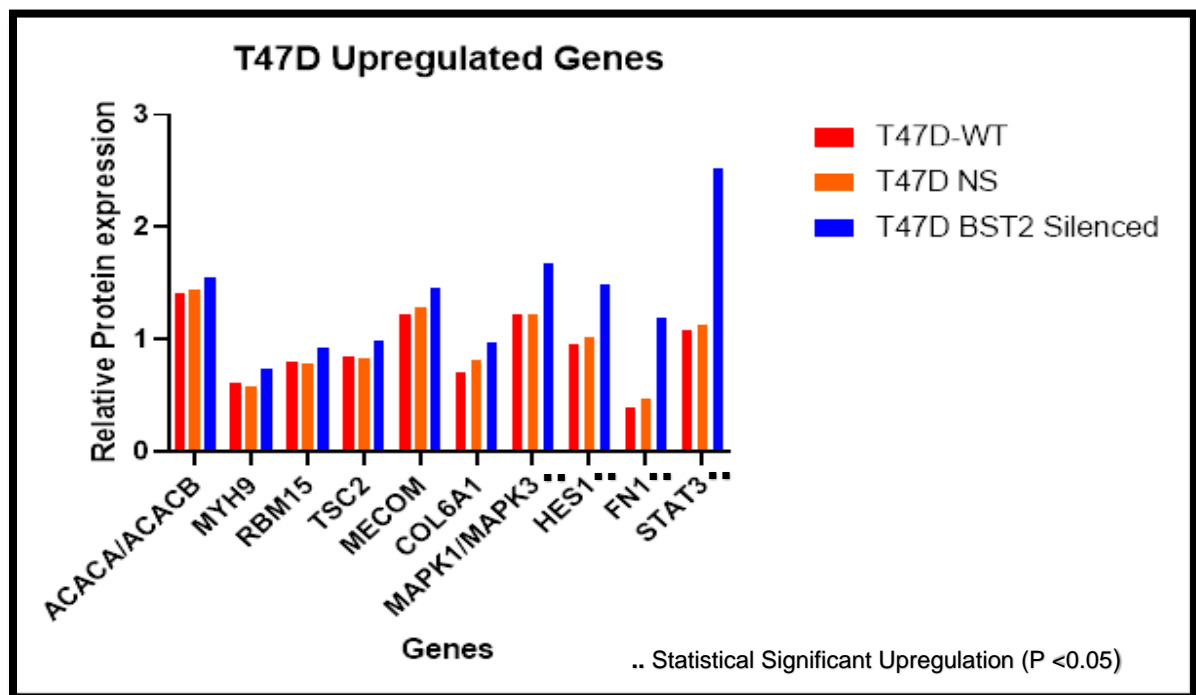


**Figure 3.23 T47D upregulated genes after BST2 silencing.**

This figure compares the level of protein expression of 10 genes among the T47D-WT (red), T47D-NS (orange), and T47D BST2-silenced (Blue) cell lines. There was a statistically significant upregulation of the following genes with the silencing of BST2: MAPK1/MAPK3, HES1, FN1 and STAT3 ( $p$  value  $< 0.05$ ).

In contrast, no statistically significant downregulation of genes was observed with BST2 silencing (Figure 3.24).

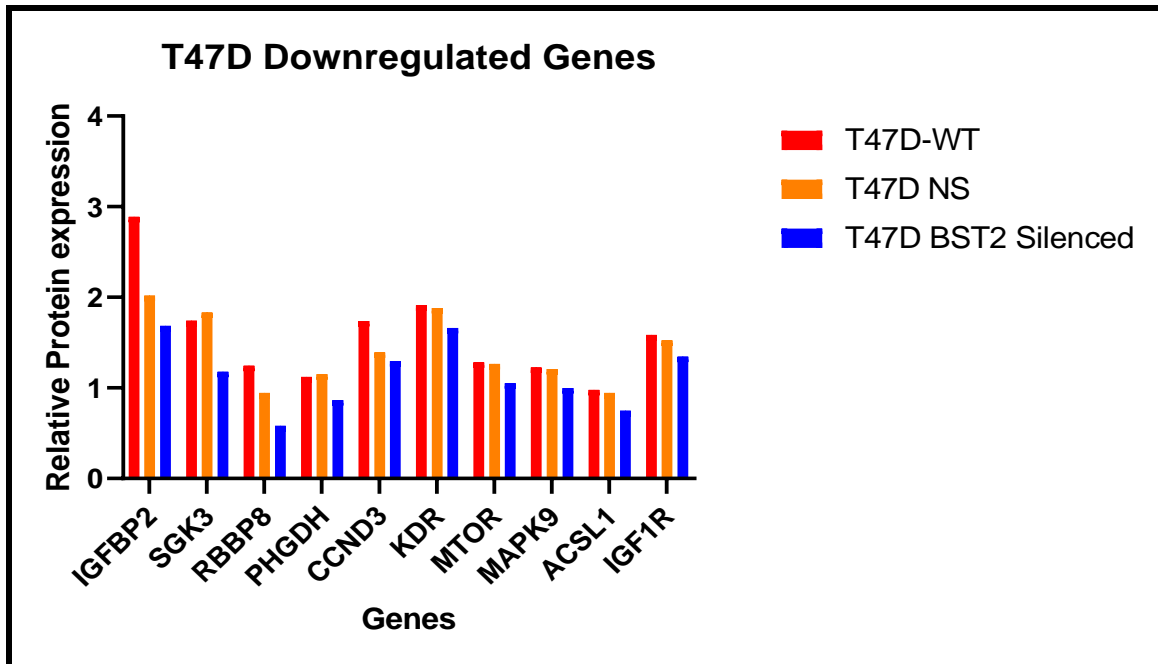


**Figure 3.24 T47D downregulated genes after BST2 Silencing.**

This figure compares the level of protein expression of 10 genes among the T47D-WT (red), T47D-NS (orange) and T47D-BST2 silenced (blue) cell lines. There was no statistically significant downregulation after silencing the BST2 gene.

## **4. Discussion & Future Directions**

### **4.1 Discussion**

Since the introduction of the hybridoma technique by Nobel prize winners Georges Kohler and Cesar Milstein in 1975, the production and utilization of monoclonal antibodies have faced several challenges, mostly related to their immunogenicity, efficacy, and toxicity (36, 37). As of 2018, a list of 29 MABs have been approved by the Food and Drug Administration for the treatment of various cancers (37) and the list is expected to grow as more cellular targets are being discovered. These cellular targets could be unique to malignant cells or simply overexpressed in cancers (38). However, the uniqueness or overexpression of a cellular target cannot predict the usefulness of a generated MAB. The distribution and density of a cellular target, as well as the possibility of variation in the target affinity, should be analyzed in both the tumor and the cross-reacting normal tissues. The excessive reactivity of MABs with normal tissues may significantly reduce the biodistribution of the therapeutic agent and negatively impact intratumoral distribution. Moreover, this excessive reactivity may increase the potential to induce severe toxic effects (39). In 2001, a phase I clinical study was conducted to examine the efficacy of anti-BST2 MAB in the treatment of multiple myeloma patients. The poor response rate was attributed to “probably diminished activity of effector cells in this heavily pretreated patient population” (25); however, the widespread distribution of BST2 in tissues and organs was not recognized at that time, which may have contributed to the trial outcome. Understanding the role(s) of a particular cellular target in the process of carcinogenesis is another essential step in the success of a

therapeutic MAb (40). The role of BST2 in carcinogenesis of various organs has not yet been fully elucidated. Furthermore, the discovery of different isoforms with distinct signaling activities, via the NF-kappa B pathway (28), have led us to study this cellular target. Based on the hypothesis, we believed that further analysis of the expression of BST2 isoforms in various cells and tissues could provide a better understanding of their role(s) in carcinogenesis, thereby offering an opportunity to recognize BST2 isoforms as potential targets for diagnostic and/or therapeutic MAbs.

In my study, I successfully generated a MAb that targets the long isoform of BST2, as described by its Japanese inventors, Jun Ohkawa and Yumiko Kakogawa (patent no. JP2004173767, 2005). Prior to the selection and production of the anti-BST2-long MAb, 563 clones went through extensive screening experiments that consecutively narrowed down the list of the potential candidates to a single clone, namely LA5. Although the final list had three clones (LA1, LA5 and BM7), the selection of LA5 was based on a combination of MAb specificity and binding affinity to the long isoform of BST2 expressed by the HEK293-long transfectant and not the transfectant expressing the medium isoform of BST2, i.e. HEK293-medium. Using anti-BST2-long MAb (clone LA5), FACS staining of HEK293 transfectants demonstrated slight insignificant binding to the medium isoform. This might be attributed to the fact that the sequence of the peptide used for mice immunization minimally overlapped with the amino acid sequence of the medium isoform. Upon designing the peptide for immunization, targeting the extracellular domain of the long isoform of BST2 and maintaining an optimal length (for the purpose of

immunogenicity) were taken into consideration. While not part of the main antigenic determinant of the peptide (RENQVLSVRI), the first five amino acids of the synthetic peptide (at the amino terminal) could be responsible for the minimal reactivity of the MAb with the medium isoform of BST2. Regardless, LA5 MAb demonstrated superiority in selectively binding to the long isoform of BST2, when compared to anti-BST2 clone 26F8 MAb, an antibody previously developed by our laboratory that recognizes all isoforms. LA5 offered an excellent method to examine my hypothesis of preferential expression of BST2 isoforms.

In terms of their affinity to the BST2 protein, the kinetic assays performed on the LA5 and 26F8 MAbs showed comparable results. LA5 MAb had a nanomolar value for the equilibrium dissociation constant ( $K_D$ ), indicating a high affinity to BST2 molecules. This feature may allow the use of LA5 MAbs as a valuable diagnostic tool to detect the expression of the long isoform of BST2 in various in-vitro assays and immunohistochemistry staining. While it is an important criterion for a good antibody, this nanomolar value of affinity may also limit the therapeutic potential of LA5 MAbs, especially for solid tumors. Adams et al. found that tumor retention of monoclonal antibodies plateaued at higher affinities (more than  $1 \times 10^{-9}$  M) and were associated with lower tumor: blood ratios (41). The combination of this level of affinity and high interstitial pressure, a common feature in many solid tumors, may create the “binding site barrier effect” that can significantly impede the transport of MAbs from the blood vessels deep into the tumor. With a higher affinity to a specific target on cancer cells, MAbs may competently bind to the perivascular cancer cells, but intratumor penetration will be progressively hampered, preventing the homogeneous

distribution of the MAb within the tumor mass (41, 42). Measuring the affinity of LA5 MAb interaction with BST2 receptors expressed on cells, instead of BST2 protein, could provide more insight into the kinetics of this interaction. Results from the specificity assays strongly indicated the high specificity of clone LA5 MAb to bind to its target, the long isoform of BST2.

After characterizing the generated MAb, I examined my hypothesis of the preferential expression of the long isoform of BST2 on cancerous cells via flow cytometry assays on various cell lines and immunohistochemistry staining of patient-derived samples of breast cancer. By comparing the flow cytometry staining of B cell lines using LA5 and 26F8 MAbs, we were able to confirm long isoform expression in the B cell lineage, as the percentages of stained cells were identical. However, the results did not reveal a differential staining between the transformed B-LCL (used as a surrogate for normal B cells) and malignant B cell lines. Several possibilities could explain the FACS data; as discussed previously, the generated anti-BST2-long LA5 MAb has minimal cross-reactivity with the HEK293 medium isoform cells (0.3% stained cells) and the generation of an antibody specific for the medium isoform could clarify this issue. Moreover, B-LCL, a non-malignant B cell line that has been transformed by the in-vitro infection of resting B cells with Epstein-Barr virus, was used as a surrogate for normal B cells. While this cell line could be a reliable source for “normal” B cells for testing carcinogen sensitivity and DNA repair (43), it might not be suitable to examine the expression of BST2 isoforms in “normal” tissues. Repeating the assay with human peripheral blood B cells would be recommended. In addition, the double staining of these cells with LA5 and 26F8 directly conjugated

to different fluorochromes and confocal microscopy analysis to examine isoforms colocalization could help in the elucidation of this observation. On the other hand, both non-malignant (MCF-10A) and malignant (MDA-MB-231, T47D and MCF7) breast epithelial cell lines stained poorly with LA5 MAb in the FACS assay. This poor staining could be secondary to technical aspects. As adherent cell lines, the breast tissue cell lines were detached with trypsin. Trypsinization might be associated with the destruction of the BST2 epitope recognized by LA5; alternative detachment solutions should thus be attempted. A low concentration of LA5 might also be inadequate for efficient staining; a serial higher concentration might reveal an increase in the mean fluorescence or staining percentage in FACS and would be suggested. Regardless, the clone LA5 demonstrated superiority over anti-BST2 clone 26F8 in the immunohistochemistry staining of breast ductal adenocarcinoma. The 26F8 MAb was associated with staining of both normal and malignant cells expressing BST2 in the analyzed tumor tissue sections. In contrast, the LA5 MAb demonstrated the capability to recognize and stain malignant ductal cells while excluding normal cells. This differentiation pattern in staining was observed while malignant ductal cells infiltrated normal acinar tissues or were surrounded by normal ductal tissues. While this observation strongly suggests the ability of the LA5 MAb to successfully identify malignant infiltration in breast cancers in immunohistochemistry assay at certain conditions and concentrations, it cannot be interpreted as solid proof of the preferential expression of the long isoform of BST2 in breast tissue malignancies. Moreover, it is well known that formalin-fixed paraffin embedded tissues expose epitopes from molecules that otherwise cannot be detected, for

instance, in native conditions such as in FACS assays. Cai et al. reported an upregulation of BST2 expression in breast cancer (20) and Mahauad-Fernandez et al. attributed this overexpression to a hypomethylation at the BST2 gene level (21). This BST2 overexpression might be a factor that enabled the LA5 MAb to detect only malignant cells, while missing normal cells. Additionally, it is not uncommon that certain antibodies are suitable for tissue staining and not for FACS, due to a different exposure of the epitope under tissue manipulations. Regardless, clone LA5 could be considered a valuable addition in breast cancer diagnostics. The ability of LA5 MAbs to detect cancer cells embedded in normal tissues within patient samples might increase the sensitivity and specificity during pathology examination. Moreover, this MAb might be helpful in confirming negative or clear margins, following surgical removal of malignancy. This anti-BST2-long (clone LA5) MAb It might also be examined on specimens of other cancers, e.g. head and neck, liver, ovarian and colorectal cancers, as these malignancies are associated with the overexpression of BST2.

To further explore the roles of BST2 in breast tissue malignancies, a loss-of-function approach with BST2-targeting short hairpin RNA (shRNA) was used. BST2 Silencing was associated with a statistically significant reduction in the viability of the T47D cell line, and no variation in proliferative ability was observed. While Cai et al. used a gain-of-function approach to study BST2 in breast cancer, they noticed an increase in the S-phase cell population (an indicator of proliferation) with the introduction of BST2 to the MDA-MB-231 breast cancer cell line (20). In another study, Mahauad-Fernandez et al. reported a reduced viability of both the MDA-MB-



231 cell line and circulating tumor cells with the suppression of BST2, as it rendered the cells susceptible to anoikis (21).

Variations in gene expression as a consequence of BST2 silencing were studied in the T47D cell line, with the view to assess the adaptive cellular response. Among the 466 genes analyzed via RPPA, only four genes demonstrated statistically significant changes. Notably, STAT3 demonstrated a significant upregulation following BST2 silencing in our assays. The signal transducer and activator of transcription 3 (STAT3) has many physiological roles in relation to several cytokines and growth factors, but it also has carcinogenic roles, especially in tumor initiation and progression. In their study of STAT3 in breast cancer, Segatto et al. observed STAT3 signaling in breast cancer cells in response to treatment. This STAT3 activation mediates survival and dormancy states, supporting the formation of locally recurrent and/or distant metastatic disease (44). This finding could point to the therapeutic use of anti-BST2 MAbs causing recurrence in breast cancer. While STAT3 overexpression with BST2 silencing might be nonspecific, it clearly indicates the significant role of BST2 in breast tumorigenesis. Other significantly overexpressed genes after BST2 silencing were MAPK1/MAPK3 and HES1. Si et al. found that overexpression of MAPK1 in breast cancer cells was associated with enhanced proliferation and chemotherapeutic resistance (45). Hairy and enhancer of split homolog-1 (HES1), a transcriptional repressor, has multiple physiological roles in cellular differentiation, apoptosis, and cell cycle arrest; overexpression of this gene was found in different malignancies, including lung, ovarian and colorectal cancers. Li et al. reported an enhanced survival and proliferation of the MCF7 breast

cancer cell line with the induced expression of HES1 (46). These findings might explain why no changes in the proliferation of T47D cells were observed with BST2 silencing. Lastly, FN1, a glycoprotein involved in cellular adhesion and migration, was significantly overexpressed after BST2 silencing. A study conducted by Yang et al. reported enhanced invasion and migration capabilities of the MCF7 cell line with the upregulation of FN1, as well as an increased resistance to chemotherapy (doxorubicin) (47). Therefore, FN1 upregulation may suggest more aggressive behavior in the T47D cell line in response to BST2 silencing. To summarize, the upregulation of these genes demonstrated the adaptive response that breast cancer cells might reveal with targeting BST2. It is also an example of the different survival mechanisms that the tumor cells may use should a critical pathway become compromised.

Finally, the minimal reactivity of the generated MAb to the HEK293 transfectant expressing the medium isoform could be considered a limitation of the generated MAb. Designing a new peptide immunogen that is shorter and modified with fluorocarbon to enhance immunogenicity could be helpful in generating MAbs with no binding to the medium isoform.

To conclude, a new MAb called LA5 was generated against the long isoform of BST2, a molecule highly expressed in several tumor types. Staining of malignant B cell lines using the new antibody confirmed the specific expression of the long isoform of BST2 in malignant B cell lines, although further experiments are required to analyze if the expression is restricted to cancer cells or not. Moreover, the LA5 MAb demonstrated potential diagnostic value that can be used to detect early

infiltration of malignant breast ductal carcinoma in patient samples. Lastly, this study provided insight about variations in gene expression in breast cancer cells with BST2 silencing. While these changes might potentially enhance the survival and proliferation of malignant cells, further research is required to validate these observations.

## 4.2 Future Directions

Identifying a cancer-specific cellular target is a critical factor that can assist in creating a successful path for target therapies. Given its widespread distribution and the vital roles it plays in the carcinogenesis of multiple tissues and organs, more advanced studies on the isoforms of BST2 should be conducted. In particular, describing the distribution of BST2 isoforms in the various organs and tissues, as well as the factors and conditions responsible for the expression and predominance of a single isoform over another, could lead to a better understanding of this protein and define the reliability of using BST2 for potential target therapy. Since these isoforms are based on posttranscriptional modifications, approaching these research questions through bioinformatics and RNA-Seq data could be helpful.

Using the monoclonal antibody approach, expression of the long BST2 isoform in other cell lines and patient samples should be explored. Several tumors reveal an elevated expression of BST2, and representative cell lines could be examined through flow cytometry assays with anti-BST2-long (clone LA5) MAbs. Employing immunohistochemistry to test the potential diagnostic value of the generated MAb on other cancers, e.g. head and neck, liver, ovarian and colorectal, is also recommended.

## **Bibliography**

1. Andrew AJ, Miyagi E, Kao S, Strebel K. The formation of cysteine-linked dimers of BST-2/tetherin is important for inhibition of HIV-1 virus release but not for sensitivity to Vpu. *Retrovirology*. 2009;6:80. Epub 2009/09/10. doi: 10.1186/1742-4690-6-80. PubMed PMID: 19737401; PMCID: PMC2754425.
2. Goto T, Kennel SJ, Abe M, Takishita M, Kosaka M, Solomon A, Saito S. A novel membrane antigen selectively expressed on terminally differentiated human B cells. *Blood*. 1994;84(6):1922-30. Epub 1994/09/15. PubMed PMID: 8080996.
3. Ishikawa J, Kaisho T, Tomizawa H, Lee BO, Kobune Y, Inazawa J, Oritani K, Itoh M, Ochi T, Ishihara K, et al. Molecular cloning and chromosomal mapping of a bone marrow stromal cell surface gene, BST2, that may be involved in pre-B-cell growth. *Genomics*. 1995;26(3):527-34. Epub 1995/04/10. doi: 10.1016/0888-7543(95)80171-h. PubMed PMID: 7607676.
4. Neil SJ, Zang T, Bieniasz PD. Tetherin inhibits retrovirus release and is antagonized by HIV-1 Vpu. *Nature*. 2008;451(7177):425-30. Epub 2008/01/18. doi: 10.1038/nature06553. PubMed PMID: 18200009.
5. OriGene Technologies I. BST2 Mouse Monoclonal Antibody [Clone ID: 2E2] 2018 [December 15, 2019]. Available from: <https://www.origene.com/catalog/antibodies/primary-antibodies/ta337180/bst2-mouse-monoclonal-antibody-clone-id-2e2>.
6. Billcliff PG, Gorleku OA, Chamberlain LH, Banting G. The cytosolic N-terminus of CD317/tetherin is a membrane microdomain exclusion motif. *Biology*

open. 2013;2(11):1253-63. Epub 2013/11/19. doi: 10.1242/bio.20135793. PubMed PMID: 24244863; PMCID: PMC3828773.

7. Dube M, Bego MG, Paquay C, Cohen EA. Modulation of HIV-1-host interaction: role of the Vpu accessory protein. *Retrovirology*. 2010;7:114. Epub 2010/12/24. doi: 10.1186/1742-4690-7-114. PubMed PMID: 21176220; PMCID: PMC3022690.

8. Kupzig S, Korolchuk V, Rollason R, Sugden A, Wilde A, Banting G. Bst-2/HM1.24 is a raft-associated apical membrane protein with an unusual topology. *Traffic (Copenhagen, Denmark)*. 2003;4(10):694-709. Epub 2003/09/06. doi: 10.1034/j.1600-0854.2003.00129.x. PubMed PMID: 12956872.

9. Schroder K, Hertzog PJ, Ravasi T, Hume DA. Interferon-gamma: an overview of signals, mechanisms and functions. *Journal of leukocyte biology*. 2004;75(2):163-89. Epub 2003/10/04. doi: 10.1189/jlb.0603252. PubMed PMID: 14525967.

10. Yoo H, Park SH, Ye SK, Kim M. IFN-gamma-induced BST2 mediates monocyte adhesion to human endothelial cells. *Cellular immunology*. 2011;267(1):23-9. Epub 2010/11/26. doi: 10.1016/j.cellimm.2010.10.011. PubMed PMID: 21094940.

11. Takeda E, Nakagawa S, Nakaya Y, Tanaka A, Miyazawa T, Yasuda J. Identification and functional analysis of three isoforms of bovine BST-2. *PloS one*. 2012;7(7):e41483. Epub 2012/08/23. doi: 10.1371/journal.pone.0041483. PubMed PMID: 22911799; PMCID: PMC3401110.

12. Cao W, Bover L. Signaling and ligand interaction of ILT7: receptor-mediated regulatory mechanisms for plasmacytoid dendritic cells. *Immunological reviews*.

2010;234(1):163-76. Epub 2010/03/03. doi: 10.1111/j.0105-2896.2009.00867.x.

PubMed PMID: 20193018; PMCID: PMC2919054.

13. Urata S, Kenyon E, Nayak D, Cubitt B, Kurosaki Y, Yasuda J, de la Torre JC, McGavern DB. BST-2 controls T cell proliferation and exhaustion by shaping the early distribution of a persistent viral infection. *PLoS pathogens*.

2018;14(7):e1007172. Epub 2018/07/22. doi: 10.1371/journal.ppat.1007172.

PubMed PMID: 30028868; PMCID: PMC6080785.

14. Arias JF, Heyer LN, von Bredow B, Weisgrau KL, Moldt B, Burton DR, Rakasz EG, Evans DT. Tetherin antagonism by Vpu protects HIV-infected cells from antibody-dependent cell-mediated cytotoxicity. *Proceedings of the National Academy of Sciences of the United States of America*. 2014;111(17):6425-30. Epub 2014/04/16. doi: 10.1073/pnas.1321507111. PubMed PMID: 24733916; PMCID: PMC4035966.

15. Edgar JR, Manna PT, Nishimura S, Banting G, Robinson MS. Tetherin is an exosomal tether. *eLife*. 2016;5. Epub 2016/09/23. doi: 10.7554/eLife.17180. PubMed PMID: 27657169; PMCID: PMC5033606.

16. Erikson E, Adam T, Schmidt S, Lehmann-Koch J, Over B, Goffinet C, Harter C, Bekeredjian-Ding I, Sertel S, Lasitschka F, Keppler OT. In vivo expression profile of the antiviral restriction factor and tumor-targeting antigen CD317/BST-2/HM1.24/tetherin in humans. *Proceedings of the National Academy of Sciences of the United States of America*. 2011;108(33):13688-93. Epub 2011/08/03. doi: 10.1073/pnas.1101684108. PubMed PMID: 21808013; PMCID: PMC3158195.

17. Atlas THP. HUMAN PROTEIN ATLAS SUMMARY 2019 [December 26, 2019]; Version 19.1:[Available from:  
<https://www.proteinatlas.org/ENSG00000130303-BST2>.
18. Wang W, Nishioka Y, Ozaki S, Jalili A, Abe S, Kakiuchi S, Kishuku M, Minakuchi K, Matsumoto T, Sone S. HM1.24 (CD317) is a novel target against lung cancer for immunotherapy using anti-HM1.24 antibody. *Cancer immunology, immunotherapy* : CII. 2009;58(6):967-76. Epub 2008/11/04. doi: 10.1007/s00262-008-0612-4. PubMed PMID: 18979097.
19. Kampf C, Olsson I, Ryberg U, Sjostedt E, Ponten F. Production of tissue microarrays, immunohistochemistry staining and digitalization within the human protein atlas. *Journal of visualized experiments : JoVE*. 2012(63). Epub 2012/06/13. doi: 10.3791/3620. PubMed PMID: 22688270; PMCID: PMC3468196.
20. Cai D, Cao J, Li Z, Zheng X, Yao Y, Li W, Yuan Z. Up-regulation of bone marrow stromal protein 2 (BST2) in breast cancer with bone metastasis. *BMC cancer*. 2009;9:102. Epub 2009/04/03. doi: 10.1186/1471-2407-9-102. PubMed PMID: 19338666; PMCID: PMC2674058.
21. Mahauad-Fernandez WD, Naushad W, Panzner TD, Bashir A, Lal G, Okeoma CM. BST-2 promotes survival in circulation and pulmonary metastatic seeding of breast cancer cells. *Scientific reports*. 2018;8(1):17608. Epub 2018/12/06. doi: 10.1038/s41598-018-35710-y. PubMed PMID: 30514852; PMCID: PMC6279795.
22. Mukai S, Oue N, Oshima T, Mukai R, Tatsumoto Y, Sakamoto N, Sentani K, Tanabe K, Egi H, Hinoi T, Ohdan H, Yasui W. Overexpression of Transmembrane



- Protein BST2 is Associated with Poor Survival of Patients with Esophageal, Gastric, or Colorectal Cancer. *Annals of surgical oncology*. 2017;24(2):594-602. Epub 2016/02/03. doi: 10.1245/s10434-016-5100-z. PubMed PMID: 26832883.
23. Yang LL, Wu L, Yu GT, Zhang WF, Liu B, Sun ZJ. CD317 Signature in Head and Neck Cancer Indicates Poor Prognosis. *Journal of dental research*. 2018;97(7):787-94. Epub 2018/02/28. doi: 10.1177/0022034518758604. PubMed PMID: 29486141.
24. Kuang CM, Fu X, Hua YJ, Shuai WD, Ye ZH, Li Y, Peng QH, Li YZ, Chen S, Qian CN, Huang W, Liu RY. BST2 confers cisplatin resistance via NF-kappaB signaling in nasopharyngeal cancer. *Cell death & disease*. 2017;8(6):e2874. Epub 2017/06/16. doi: 10.1038/cddis.2017.271. PubMed PMID: 28617432; PMCID: PMC5520926.
25. Harada T, Ozaki S. Targeted therapy for HM1.24 (CD317) on multiple myeloma cells. *BioMed research international*. 2014;2014:965384. Epub 2014/08/22. doi: 10.1155/2014/965384. PubMed PMID: 25143955; PMCID: PMC4124849.
26. Russell Burke ML, Dorian LaTocha, Tomohide Yamazaki, Koji Ishida, Naoko Arai, Stephen Spurgeon. Identification of BST2 as a Potential Therapeutic Target in B Cell Malignancies Including Chronic Lymphocytic Leukemia and Mantle Cell Lymphoma. *Clinical Lymphoma, Myeloma & Leukemia*. 2011;11, Supplement 2:S192 - S3. Epub October 8, 2011. doi: <https://doi.org/10.1016/j.clml.2011.09.085>.
27. Jun Ohkawa, Kamogawa Y. Methods for suppressing activity of activated interferon-producing cells2005;US8435530B2.

28. Cocka LJ, Bates P. Identification of alternatively translated Tetherin isoforms with differing antiviral and signaling activities. *PLoS pathogens*. 2012;8(9):e1002931. Epub 2012/10/03. doi: 10.1371/journal.ppat.1002931. PubMed PMID: 23028328; PMCID: PMC3460627.
29. Karin M. Nuclear factor-kappaB in cancer development and progression. *Nature*. 2006;441(7092):431-6. Epub 2006/05/26. doi: 10.1038/nature04870. PubMed PMID: 16724054.
30. Cao W, Rosen DB, Ito T, Bover L, Bao M, Watanabe G, Yao Z, Zhang L, Lanier LL, Liu YJ. Plasmacytoid dendritic cell-specific receptor ILT7-Fc epsilonRI gamma inhibits Toll-like receptor-induced interferon production. *The Journal of experimental medicine*. 2006;203(6):1399-405. Epub 2006/06/01. doi: 10.1084/jem.20052454. PubMed PMID: 16735691; PMCID: PMC2118323.
31. Cao W, Bover L, Cho M, Wen X, Hanabuchi S, Bao M, Rosen DB, Wang YH, Shaw JL, Du Q, Li C, Arai N, Yao Z, Lanier LL, Liu YJ. Regulation of TLR7/9 responses in plasmacytoid dendritic cells by BST2 and ILT7 receptor interaction. *The Journal of experimental medicine*. 2009;206(7):1603-14. Epub 2009/07/01. doi: 10.1084/jem.20090547. PubMed PMID: 19564354; PMCID: PMC2715090.
32. Bio F. High throughput Octet HTX and Octet RED384 Systems 2020 [March 5, 2020]. Available from: <https://www.fortebio.com/products/label-free-bli-detection/high-throughput-octet-systems>.
33. Kamala T. Hock immunization: a humane alternative to mouse footpad injections. *Journal of immunological methods*. 2007;328(1-2):204-14. Epub

2007/09/07. doi: 10.1016/j.jim.2007.08.004. PubMed PMID: 17804011; PMCID: PMC2464360.

34. Lopez-Mosqueda J, Maddi K, Prgomet S, Kalayil S, Marinovic-Terzic I, Terzic J, Dikic I. SPRTN is a mammalian DNA-binding metalloprotease that resolves DNA-protein crosslinks. *eLife*. 2016;5. Epub 2016/11/18. doi: 10.7554/eLife.21491. PubMed PMID: 27852435; PMCID: PMC5127644.

35. Complete sequencing and characterization of 21,243 full-length human cDNAs [Internet]2004 [cited March 9, 2020]. Available from: [https://www.ncbi.nlm.nih.gov/protein/NP\\_114407.3](https://www.ncbi.nlm.nih.gov/protein/NP_114407.3).

36. Buss NA, Henderson SJ, McFarlane M, Shenton JM, de Haan L. Monoclonal antibody therapeutics: history and future. *Current opinion in pharmacology*. 2012;12(5):615-22. Epub 2012/08/28. doi: 10.1016/j.coph.2012.08.001. PubMed PMID: 22920732.

37. Kimiz-Gebologlu I, Gulce-Iz S, Biray-Avci C. Monoclonal antibodies in cancer immunotherapy. *Molecular biology reports*. 2018;45(6):2935-40. Epub 2018/10/13. doi: 10.1007/s11033-018-4427-x. PubMed PMID: 30311129.

38. Pento JT. Monoclonal Antibodies for the Treatment of Cancer. *Anticancer research*. 2017;37(11):5935-9. Epub 2017/10/25. doi: 10.21873/anticanres.12040. PubMed PMID: 29061772.

39. Beckman RA, Weiner LM, Davis HM. Antibody constructs in cancer therapy: protein engineering strategies to improve exposure in solid tumors. *Cancer*. 2007;109(2):170-9. Epub 2006/12/13. doi: 10.1002/cncr.22402. PubMed PMID: 17154393.

40. Stern M, Herrmann R. Overview of monoclonal antibodies in cancer therapy: present and promise. *Critical reviews in oncology/hematology*. 2005;54(1):11-29. Epub 2005/03/23. doi: 10.1016/j.critrevonc.2004.10.011. PubMed PMID: 15780905.
41. Adams GP, Schier R, McCall AM, Simmons HH, Horak EM, Alpaugh RK, Marks JD, Weiner LM. High affinity restricts the localization and tumor penetration of single-chain fv antibody molecules. *Cancer research*. 2001;61(12):4750-5. Epub 2001/06/19. PubMed PMID: 11406547.
42. Jain RK, Baxter LT. Mechanisms of heterogeneous distribution of monoclonal antibodies and other macromolecules in tumors: significance of elevated interstitial pressure. *Cancer research*. 1988;48(24 Pt 1):7022-32. Epub 1988/12/15. PubMed PMID: 3191477.
43. Hussain T, Mulherkar R. Lymphoblastoid Cell lines: a Continuous in Vitro Source of Cells to Study Carcinogen Sensitivity and DNA Repair. *International journal of molecular and cellular medicine*. 2012;1(2):75-87. Epub 2012/04/01. PubMed PMID: 24551762; PMCID: PMC3920499.
44. Segatto I, Baldassarre G, Belletti B. STAT3 in Breast Cancer Onset and Progression: A Matter of Time and Context. *International journal of molecular sciences*. 2018;19(9). Epub 2018/09/21. doi: 10.3390/ijms19092818. PubMed PMID: 30231553; PMCID: PMC6163512.
45. Si W, Shen J, Du C, Chen D, Gu X, Li C, Yao M, Pan J, Cheng J, Jiang D, Xu L, Bao C, Fu P, Fan W. A miR-20a/MAPK1/c-Myc regulatory feedback loop regulates breast carcinogenesis and chemoresistance. *Cell death and differentiation*.

2018;25(2):406-20. Epub 2017/11/11. doi: 10.1038/cdd.2017.176. PubMed PMID: 29125598; PMCID: PMC5762853.

46. Li X, Cao Y, Li M, Jin F. Upregulation of HES1 Promotes Cell Proliferation and Invasion in Breast Cancer as a Prognosis Marker and Therapy Target via the AKT Pathway and EMT Process. *Journal of Cancer*. 2018;9(4):757-66. Epub 2018/03/21. doi: 10.7150/jca.22319. PubMed PMID: 29556333; PMCID: PMC5858497.

47. Yang X, Hu Q, Hu LX, Lin XR, Liu JQ, Lin X, Dinglin XX, Zeng JY, Hu H, Luo ML, Yao HR. miR-200b regulates epithelial-mesenchymal transition of chemo-resistant breast cancer cells by targeting FN1. *Discovery medicine*. 2017;24(131):75-85. Epub 2017/10/04. PubMed PMID: 28972876.

## **Vita**

Ahmed Muhsin was born in Ames, Iowa, the son of Professor Mohammed Muhsin and Ahlam Naji. In 1986, he went back to Iraq where he completed middle and high school in the Gifted Boys' School in Baghdad. In 1997, he started medical school at the University of Al-Mustansiriyah. After graduation in 2003, he practiced medicine in Iraq and Australia. In 2015, he joined Texas A&M School of public health as a Master of Public Health (MPH) student. While there, he worked as a research assistant on several projects. In Fall 2017, he started his Master of Science degree with a concentration in Cancer Biology at The University of Texas MD Anderson Cancer Center UTHHealth Graduate School of Biomedical Sciences. In Fall 2020, he will start his Ph.D. in medical sciences at Texas A&M Institute of Biosciences and technology in Houston, Texas.

Permanent address:

14811 Wayson Drive

Sugar Land, Texas 77498